

On the polarizability and capacitance of the cube*

Johan Helsing and Karl-Mikael Perfekt
Centre for Mathematical Sciences
Lund University, P.O. Box 118, SE-221 00 Lund, Sweden

March 14, 2019

Abstract

An efficient integral equation based solver is constructed for the electrostatic problem on domains with cuboidal inclusions. It can be used to compute the polarizability of a dielectric cube in a dielectric background medium at virtually every permittivity ratio for which it exists. For example, polarizabilities accurate to between five and ten digits are obtained (as complex limits) for negative permittivity ratios in minutes on a standard workstation. In passing, the capacitance of the unit cube is determined with unprecedented accuracy. With full rigor, we develop a natural mathematical framework suited for the study of the polarizability of Lipschitz domains. Several aspects of polarizabilities and their representing measures are clarified, including limiting behavior both when approaching the support of the measure and when deforming smooth domains into a non-smooth domain. The success of the mathematical theory is achieved through symmetrization arguments for layer potentials.

1 Introduction

The determination of polarizabilities and capacitances of inclusions of various shapes has a long history in computational electromagnetics. Inclusions with smooth surfaces are, by now, rather standard to treat. When surfaces are non-smooth, however, the situation is different. Numerical solvers can run into problems related to stability and resolution. Particularly so in three dimensions and for certain permittivity combinations. Solutions may not converge or results could be hard to interpret. See [47, 48, 54] and references therein. The situation on the theoretical side is similar. When, and in what sense do solutions exist? Such questions are in the mainstream of contemporary research in harmonic analysis. Coincidentally, also in applied physics (plasmonics) there is a growing interest in solving electrostatic

*Supported by the Swedish Research Council under contract 621-2011-5516.

problems on domains with structural discontinuities and a concern about the sufficiency of available solvers [21, 56].

This paper addresses several fundamental issues related to the problems just mentioned. We construct a stable solver for the polarizability and capacitance of a cube based on an integral equation using the adjoint of the double layer potential. We compute solutions of unprecedented accuracy and interpret the results within a rigorous mathematical framework. The reason for working with a cube are twofold. First, the cube has the advantage that its geometric difficulties are concentrated to edges and corners, since its faces are flat. Integral equation techniques, which often excel for boundary value problems in two dimensions, typically suffer from loss of accuracy in the discretization of weakly singular integral operators on curved surfaces in three dimensions. Here we need not worry about that. Secondly, cubes are actually common in plasmonic applications.

In the purely theoretical sections we begin by collecting a number of results and recent advances in the theory of layer potentials associated with the Laplacian in Lipschitz domains. The most obvious reason for this is that the invertibility study of layer potentials leads to the solution of the boundary value problem implicit in the definition of polarizability, and is as such the basis for both the mathematical and numerical aspects of this paper. Furthermore, the properties of the polarizability for a non-smooth domain such as a cube are quite subtle, and it is our ambition to provide a solid theoretical foundation for the problem at hand, giving a careful and detailed exposition of a mathematical framework that clarifies a number of points.

Since the double layer potential is not self-adjoint in the L^2 -pairing, we develop certain symmetrization techniques for it, in particular extending the work of Khavinson, Putinar and Shapiro [35] to the case of a non-smooth domain. These techniques are used to prove the unique existence of the polarizability itself for a Lipschitz domain, as well as of a corresponding representing measure [20]. We present a thorough discussion of the smooth case, the limiting behavior in passing from the smooth to the non-smooth case, and ultimately the general case. Concerning the last point, a condition ensuring that the representing measure has no singular part is given, and it is proven that in the support of the absolutely continuous part of the measure, the polarizability can not be given a direct interpretation in terms of a potential with finite energy solving the related boundary value problem.

The paper is organized as follows: Section 2 formulates the electrostatic problem and defines the polarizability. Existence issues and representations are reviewed in Section 3. For ease of reading, rigorous statements and proofs are deferred to Sections 4 and 5. The capacitance is discussed in Section 6. Section 7 reviews the state of the art with regard to numerical schemes. Section 8 gives a necessary background to the present solver. New development takes place in Section 9. The last sections contain nu-

merical examples performed in MATLAB. Section 10 illustrates the effects of rounding corners and Section 11 is about the cube.

The main conclusion of the paper is that, from a numerical viewpoint, it is an advantage to let cubes have sharp edges and corners as opposed to the common practice of rounding them slightly. Furthermore, the representing measure for the polarizability of the cube is determined, and a new benchmark for the capacitance of the unit cube is established.

2 The electrostatic problem and the polarizability

Let a domain V , an inclusion with surface S and permittivity ϵ_2 , be embedded in an infinite space. The exterior to the closure of V is denoted E and has permittivity ϵ_1 . Let ν_r be the exterior unit normal of S at position r .

We seek a potential $U(r)$, continuous in $E \cup S \cup V$, which satisfies the electrostatic equation

$$\Delta U(r) = 0, \quad r \in E \cup V, \quad (1)$$

subject to the boundary conditions on the limits of normal derivatives

$$\epsilon_1 \frac{\partial}{\partial \nu_r} U^{\text{ext}}(r) = \epsilon_2 \frac{\partial}{\partial \nu_r} U^{\text{int}}(r) \quad (2)$$

and behavior at infinity

$$\lim_{r \rightarrow \infty} \nabla U(r) = e. \quad (3)$$

Here superscripts ext and int denote limits from the exterior or interior of S , respectively, and e is an applied unit field. Eqs. (1), (2), (3) constitute a partial differential equation formulation of the electrostatic problem. Proposition 5.1 gives a strict interpretation of what it means for a potential $U(r)$ to solve this problem, in particular expressing (2) in a distribution sense.

For the construction of solutions to (1), (2), (3) we make use of fundamental solutions to the Laplace equation in two and three dimensions

$$G(r, r') = -\frac{1}{2\pi} \log |r - r'| \quad \text{and} \quad G(r, r') = \frac{1}{4\pi} \frac{1}{|r - r'|}, \quad (4)$$

and represent $U(r)$ in terms of a single layer density $\rho(r)$ as

$$U(r) = e \cdot r + \int_S G(r, r') \rho(r') d\sigma_{r'}, \quad (5)$$

where $d\sigma$ is an element of surface area.

The representation (5) satisfies (1) and (3). Its insertion in (2) gives the integral equation for $\rho(r)$

$$\rho(r) + 2\lambda \int_S \frac{\partial}{\partial \nu_r} G(r, r') \rho(r') d\sigma_{r'} = -2\lambda (e \cdot \nu_r), \quad r \in S, \quad (6)$$

where the parameter

$$\lambda = \frac{\epsilon_2 - \epsilon_1}{\epsilon_2 + \epsilon_1}. \quad (7)$$

The polarizability tensor of V can be defined in terms of an integral over a polarization field. When V features sufficient symmetry, such as the octahedral symmetry of the cube, the polarizability is isotropic and reduces to a scalar $\alpha(\epsilon_1, \epsilon_2)$, see [51], which can be determined via

$$(\epsilon_2 - \epsilon_1) \int_V \nabla U(r) \, dr = \alpha(\epsilon_1, \epsilon_2) e, \quad (8)$$

where dr is a volume element. Using integration by parts in (8) it is possible to express $\alpha(\epsilon_1, \epsilon_2)$ as an integral over $\rho(r)$

$$\alpha(\epsilon_1, \epsilon_2) = -\epsilon_1 \int_S \rho(r) (e \cdot r) \, d\sigma_r. \quad (9)$$

More generally, the components of the polarizability tensor can be recovered via integrals similar to that in (9) using different applied fields e , but in what follows we tacitly assume that V is sufficiently symmetric as to allow for a scalar valued $\alpha(\epsilon_1, \epsilon_2)$.

3 Theory – overview

For what surface shapes S and permittivities ϵ_1, ϵ_2 does the electrostatic problem have a solution? Starting with (6) and partly following [40], this section sketches the derivation of some important existence results. It also motivates an integral representation formula for $\alpha(\epsilon_1, \epsilon_2)$ and two sum rules which are used for validation in our numerical experiments.

3.1 Existence of solutions for smooth S

Let us rewrite (6) in the abbreviated form

$$(I + \lambda K) \rho(r) = \lambda g(r), \quad (10)$$

where I is the identity. If S is smooth, then (10) is a Fredholm second kind integral equation with a compact, non-self adjoint, integral operator K whose spectrum is discrete and accumulates at zero. Let K and its adjoint K^* (the double layer potential) have eigenvectors ϕ_i and ψ_i with corresponding eigenvalues z_i . All eigenvalues are real and bounded by one in modulus. Non-zero eigenvalues have finite multiplicities. Normalizing

$$\int_S \overline{\psi_i(r)} \phi_j(r) \, d\sigma_r = \delta_{ij}, \quad (11)$$

the kernel of K can be written

$$K(r, r') = \sum_i z_i \phi_i(r) \overline{\psi_i(r')}. \quad (12)$$

See, further, the discussion in Section 5.2.

Let us introduce a new variable z and a scaled polarizability $\alpha(z)$ as

$$z = -1/\lambda, \quad (13)$$

$$\alpha(z) \equiv \frac{\alpha(\epsilon_1, \epsilon_2)}{|V|\epsilon_1}, \quad (14)$$

where $|V|$ is the volume of V . Then (14), with (9), can be written in the abbreviated form

$$\alpha(z) = \int_S h(r) \rho(r) d\sigma_r. \quad (15)$$

The relation (13) allows us to use the parameter λ or its negative reciprocal z , depending on what is most convenient in a given situation.

In terms of the quantities

$$u_i = \int_S h(r) \phi_i(r) d\sigma_r \quad \text{and} \quad v_i = \int_S \overline{\psi_i(r)} g(r) d\sigma_r, \quad (16)$$

and using (12) to construct the resolvent of (10), one can write

$$\rho(r) = \sum_i \frac{\phi_i(r) v_i}{z_i - z} \quad (17)$$

and

$$\alpha(z) = \sum_i \frac{u_i v_i}{z_i - z}, \quad (18)$$

see Theorem 5.6. This suggests that neither $U(r)$ nor $\alpha(z)$ exists for $z = z_i$ when $u_i v_i \neq 0$. There is an *electrostatic resonance* or *plasmon* at z_i .

For ease of interpretation, the sum in (18) can be considered as taken over distinct eigenvalues and with $u_i v_i$, for a degenerate eigenvalue, being the sum of all residues belonging to that eigenvalue. Then all $u_i v_i$ are non-negative and plasmons can be classified as *bright* or *dark* depending on whether $u_i v_i > 0$ or not [56]. When S is a circle, there are only two eigenvalues: $z_1 = -1$ which is simple and corresponds to a dark plasmon and $z_2 = 0$ which has infinite multiplicity and corresponds to a bright plasmon. When S is a sphere, the eigenvalues are $z_i = 1/(1 - 2i)$. The multiplicity of z_i is $2i - 1$. The only bright plasmon is associated with z_2 .

For later reference we observe that the sum of all residues is

$$\sum_i u_i v_i = \int_S h(r) g(r) d\sigma_r = 2. \quad (19)$$

When the polarizability is isotropic one can, using techniques from [17], also derive a weighted sum rule

$$\sum_i z_i u_i v_i = \int_S \int_S h(r) K(r, r') g(r') d\sigma'_r d\sigma_r = 2(2/d - 1), \quad (20)$$

where $d = 2, 3$ is the dimension.

3.2 Existence of solutions for non-smooth S

If S is gradually transformed from a smooth surface into a non-smooth surface, eigenvalues z_i travel and occupy a certain subset of the interval $[-1, 1]$ ever more densely. When S ceases to be smooth, K is no longer compact with discrete eigenvalues. Rather, K has a continuous spectrum which on a certain function space coincides with the aforementioned subset, accompanied by discrete values. Disregarding the discrete spectrum, which for squares and cubes turns out to correspond to dark plasmons, the sum (18) assumes a limit

$$\alpha(z) = \int_{\mathbb{R}} \frac{d\mu(x)}{x - z} = \int_{\sigma_\mu} \frac{\mu'(x) dx}{x - z}, \quad (21)$$

where the measure $\mu(x)$ is real and non-negative and $\sigma_\mu = \{x : \mu'(x) > 0\}$. Here we have ignored the possible presence of a singular spectrum. For further details and a condition that serves to exclude this complication, see Theorems 5.2 and Section 5.2. The sum rules (19) and (20) assume the forms

$$\int_{\mathbb{R}} \mu'(x) dx = 2, \quad (22)$$

$$\int_{\mathbb{R}} x \mu'(x) dx = 2(2/d - 1). \quad (23)$$

The numerical results in Sections 10 and 11 suggest that both the square and the cube have σ_μ equal to a single, possibly punctured, interval $(a, b) \subset [-1, 1]$. The square has $a = -0.5$ and $b = 0.5$, consistent with what is obtained by letting $p \rightarrow \infty$ in eq. (4.5.60) of [32]. See also [28, Section 2] and [11, 31]. The cube has $a \approx -0.694526$ and $b = 0.5$. For later reference we let $\sigma_{\mu\text{sq}}$ denote σ_μ of the square and $\sigma_{\mu\text{cu}}$ denote σ_μ of the cube.

For a large class of non-smooth S , the potential $U(r)$ exists when z stays away from a certain compact set $L : \sigma_\mu \subset L \subset [-1, 1]$. Furthermore, $\alpha(z)$ has a limit,

$$\alpha^+(x) = \lim_{y \rightarrow 0^+} \alpha(x + iy), \quad (24)$$

as $z = x + iy$ approaches x from the upper half-plane for almost all $x \in \mathbb{R}$. See Theorem 5.2 and Section 5.2. It is important in this context and when $x \in \sigma_\mu$ not to interpret $\alpha^+(x)$ as a polarizability corresponding to a meaningful

solution $U(r)$ for a negative permittivity ratio $\epsilon_2/\epsilon_1 = (x-1)/(x+1)$. On the contrary, Theorem 5.8 states that there is no $U(r)$ with finite energy solving (1), (2), (3) when $z = x \in \sigma_\mu$. Therefore, any attempt to solve the electrostatic problem for $z \in \sigma_\mu$ is bound to fail.

3.3 The limit polarizability $\alpha^+(x)$ and its relation to $\mu'(x)$

This paper aims at constructing an efficient scheme for computing $\alpha(z)$ of a cube at all z for which this quantity exists. Still, in our numerical experiments we only compute the limit $\alpha^+(x)$ of (24) for $x \in [-1, 1]$. The reason for this is that the computation of $\alpha(z)$ is hardest for z close to $\sigma_\mu \subseteq [-1, 1]$. Accurate results for $\alpha^+(x)$ therefore indicate a robust scheme. Furthermore, there is a simple connection between $\alpha^+(x)$ and $\mu'(x)$. Using jump relations for Cauchy-type integrals one can show from (21) that

$$\mu'(x) = \Im\{\alpha^+(x)\}/\pi, \quad x \in \mathbb{R}. \quad (25)$$

Knowledge of $\mu'(x)$ for non-smooth S is of great interest in theoretical materials science. Closed form expressions seem to be out of reach, however, except for a famous example in a periodic two-dimensional setting [10, 43]. As for numerics, merely determining σ_μ is a challenge [47, 54]. To the authors' knowledge, σ_μ is not known for any S exhibiting corners in three dimensions. The accurate determination of $\mu'(x)$ is even harder [34]. Studying how (18) evolves as a smooth S becomes non-smooth is not an efficient method. Eigenvalue problems are costly to solve. The discretization of K on surface portions of high curvature is problematic. Conditioning is also an issue and details of the mapping $u_i v_i \rightarrow \mu'(x)$ need to be worked out. It is desirable to find $\mu'(x)$ in a more direct way and (25) offers precisely this. Obtaining $\mu'(x)$ is a subproblem of computing $\alpha^+(x)$ for $x \in [-1, 1]$.

4 Theory – preliminaries

Let $V \subset \mathbb{R}^d$, $d \geq 2$, be an open and bounded set that is Lipschitz, in the sense that its boundary $S = \partial V$ is connected and locally the graph of a Lipschitz function in some basis. For a more precise definition of this concept, see for example [53]. To avoid a certain technicality we will also assume that V is star-like, meaning that there exists an $r_0 \in V$ such that the line segments between r_0 and every other point $r \in V$ are contained in V . In the applications of this paper, V will take on the role of the square in \mathbb{R}^2 , the cube in \mathbb{R}^3 , or a set with smooth boundary approximating either of the two. As before we will denote $E = \overline{V}^c$.

In this section we first record a number of results about the single and double layer potentials associated with the Laplacian on V , to then introduce the mathematical framework in which we will study the boundary value

problem given by (1), (2), (3). Actually, in this section and the next, we will develop the theory only for $d \geq 3$. The two-dimensional case contains several anomalies in relation to the higher-dimensional theory, and it is for the sake of clarity and brevity that we exclude it. We shall indicate some of the differences as we progress, but we note here that the main results about the polarizability $\alpha(z)$ remain true also for $d = 2$.

While $L^2(S)$ is a natural domain for the operator K , we will primarily focus on the action of K on certain Sobolev spaces H^s . There is good reason for this. For one, K is not self-adjoint as an operator on $L^2(S)$, or even normal, so that the spectral theorem can not be directly applied. We will therefore develop certain symmetrization techniques, and these demand that we consider K on fractional Sobolev spaces. A second, related reason, is that the L^2 -spectrum of K is no longer contained in the real line when S fails to be smooth (see I. Mitrea [45]). We shall see that considering K on a Sobolev space amends this problem. We also note here that by the X -spectrum of a bounded operator T on a Hilbert space X , $T : X \rightarrow X$, we always mean the set

$$\text{Spec}(T, X) = \{z \in \mathbb{C} : K - z \text{ is not bijective on } X\}.$$

When $z \notin \text{Spec}(T, X)$ it is a consequence of the closed graph theorem that $K - z$ has a bounded inverse $(K - z)^{-1} : X \rightarrow X$.

For $s = 0$ we have simply that $H^0(V) = L^2(V)$ and $H^0(S) = L^2(S)$. For $s = 1$, $H^1(V)$ is the Hilbert space of distributions u such that u and $\partial_{x_j} u$, $1 \leq j \leq n$, are members of $L^2(V)$. The norm is given by

$$\|u\|_{H^1(V)}^2 = \|u\|_{L^2(V)}^2 + \|\nabla u\|_{L^2(V)}^2.$$

$H^1(S)$ can be defined similarly using the almost everywhere defined tangential vectors of S , see for example Geymonat [19]. For $0 < s < 1$, H^s can be defined by real interpolation methods, but in our situation it can alternatively be characterized by a Besov type norm. That is, $u \in H^s(V)$ if

$$\|u\|_{H^s(V)}^2 = \|u\|_{L^2(V)}^2 + \int_{V \times V} \frac{|u(r) - u(r')|^2}{|r - r'|^{d+2s}} dr dr' < \infty.$$

$u \in H^s(V)$ is then inductively defined for $s = s_i + s_f$ with $s_i \geq 1$ an integer and $0 < s_f \leq 1$ by requiring that $u \in H^{s_i}$ and $\partial^\beta u \in H^{s_f}$ for $\beta = (\beta_1, \dots, \beta_d)$ with $\sum \beta_k = s_i$. Returning to the case $0 < s < 1$, we have that $u \in H^s(S)$ if

$$\|u\|_{H^s(S)}^2 = \|u\|_{L^2(S)}^2 + \int_{S \times S} \frac{|u(r) - u(r')|^2}{|r - r'|^{d-1+2s}} d\sigma_r d\sigma_{r'} < \infty,$$

where σ denotes Hausdorff measure on S . See Adams [1] and Grisvard [22] for further information and the equivalence of various definitions in the

Lipschitz setting. For $s > 0$ we define H^{-s} as the dual space of H^s in the L^2 -pairing. More precisely, a distribution u lies in H^{-s} if and only if

$$\|u\|_{H^{-s}} = \sup_{\|v\|_{H^s}=1} |\langle u, v \rangle_{L^2}| < \infty.$$

We shall also make use of Sobolev traces, which give us a way to assign boundary values to distributions in V . We will only require the classical Gagliardo result [18] which says that there uniquely exists a continuous, surjective linear operator $\text{Tr} : H^1(V) \rightarrow H^{1/2}(S)$ with right continuous inverse such that $\text{Tr } u = u|_S$ for any $u \in C^\infty(\bar{V})$. There is also a corresponding trace from the exterior domain with the same properties, $\text{Tr}_E : H^1(E) \rightarrow H^{1/2}(S)$.

The $L^2(S)$ -adjoint K^* of the operator K is known as the double layer potential, given by the formula

$$(K^*u)(r) = 2 \int_S \frac{\partial}{\partial \nu_{r'}} G(r, r') u(r') d\sigma_{r'}, \quad u \in L^2(S), r \in S. \quad (26)$$

For $d = 2$ and $d = 3$ the Newtonian kernel G has already been defined in (4), and for $d > 3$ it is given by

$$G(r, r') = \omega_d |r - r'|^{2-d},$$

with a normalization constant ω_d chosen so that $\Delta_r G(r, 0) = -\delta$ in the sense of distributions. When S is a C^2 -surface the kernel of K^* is only weakly singular (for $d = 2$ there is no singularity at all present), and it is a standard matter to see that (26) defines K^* as a compact operator on $H^s(S)$ for $0 \leq s \leq 1$. The compactness of K^* makes its spectral analysis considerably easier, and in this case it is well known that

$$\text{Spec}(K^*, L^2(S)) \subset [-1, 1), \quad (27)$$

see for example the results of Escauriaza, Fabes and Verchota [13] together with the fact that the spectrum of K^* is real in the C^2 -case. This latter point will be discussed further later on.

Unfortunately, when S is only a Lipschitz surface, K^* is no longer compact in general. In fact, when S is a curvilinear polygon in two dimensions, I. Mitrea [45] has shown that the L^2 -spectrum of K^* consists of the union of certain solid “figure eights” in the complex plane, one for each (non-smooth) vertex of S , in addition to a finite number of real eigenvalues. In particular this applies when S is a square in two dimensions, with only one figure eight present, since all angles are equal. The general situation is not as well understood, but when $V \subset \mathbb{R}^d$ is convex, as it is in our situation, it is known that the spectral radius of K^* on $L^2(S)$ is 1, see Fabes, Sand and Seo [15].

To even define K^* in the general Lipschitz setting, the integral in (26) must be understood in an almost everywhere principal value sense. We

remark, however, that when S is a curvilinear polyhedron, $K^*u(r)$ can be evaluated in the usual integral sense, except possibly when r belongs to an edge of S , and so it is not necessary to consider principal values in the main applications of this paper. Proving the boundedness of K^* on $L^2(S)$ was an accomplishment of Coifman, McIntosh and Meyer [9] in their study of singular integrals. The boundedness of K^* as an operator on $H^s(S)$, $0 < s \leq 1$, also essentially follows from [9], see for example Meyer [41]. By duality we immediately obtain that K is bounded on $H^{-s}(S)$, $0 \leq s \leq 1$.

For $u \in L^2(S)$ one may of course also evaluate the integral (26) in $V \cup E$ to obtain a harmonic function. We denote

$$(Du)(r) = 2 \int_S \frac{\partial}{\partial \nu_{r'}} G(r, r') u(r') d\sigma_{r'}, \quad r \in V \cup E.$$

Fabes, Mendez and M. Mitrea [14] prove that for $0 < s < 1$, $D : H^s(S) \rightarrow H^{s+1/2}(V)$ is bounded.

The single layer potential of u , defined in all of \mathbb{R}^d , is given by

$$(\mathcal{S}u)(r) = 2 \int_S G(r, r') u(r') d\sigma_{r'}, \quad u \in L^2(S), r \in \mathbb{R}^d.$$

The kernel G is only weakly singular when S is a Lipschitz surface, so that there is no issue in defining this integral operator. In fact, \mathcal{S} has smoothening properties. D. Mitrea [44] shows that for $0 \leq s \leq 1$, $\mathcal{S} : H^{-s}(S) \rightarrow H^{1-s}(S)$ is a bicontinuous isomorphism and in [14] it is proven that \mathcal{S} is bounded as a map $\mathcal{S} : H^{-s}(S) \rightarrow H^{\frac{3}{2}-s}(V)$ for $0 < s < 1$. It is clear that \mathcal{S} is self-adjoint in the $L^2(S)$ -pairing and that $\mathcal{S}u$ is harmonic in $V \cup E$.

At this stage, a peculiarity of the case $d = 2$ appears. In any dimension, there exists uniquely a function $u_0 \in L^2(S)$ such that $(I + K)u_0 = 0$ and $\int_S u_0 d\sigma = 1$, and one can show that $\mathcal{S}u_0|_{\overline{V}} \equiv c$ is constant. In higher dimensions this constant can never be zero, but for $d = 2$ there exist domains such that $c = 0$. When this occurs \mathcal{S} clearly fails to be injective, and its range is also affected. On the other hand, if $c = 0$ for a particular domain V , any non-trivial dilation of V will give a domain with $c \neq 0$ and the properties in the previous paragraph may be proven to hold for the dilated domain, at least for $s = 1/2$, which will turn out to be the important case for us. See Verchota [53] for details. Note that since our object of interest, the polarizability $\alpha(z)$, is scaling invariant, this anomaly of \mathcal{S} for $d = 2$ presents no real obstacle.

While the kernel of \mathcal{S} is sufficiently nonsingular to immediately define a continuous function $\mathcal{S}u$ everywhere on \mathbb{R}^d if u is for example bounded, similar statements are never true for the kernel of K^* . In fact, the following

jump formulas hold for a function $u \in L^2(S)$.

$$\begin{aligned} \mathcal{S}^{\text{int}}u &= \mathcal{S}^{\text{ext}}u = \mathcal{S}u & \partial_\nu \mathcal{S}^{\text{int}}u &= u + Ku \\ \partial_\nu \mathcal{S}^{\text{ext}}u &= -u + Ku & D^{\text{int}}u &= -u + K^*u \\ D^{\text{ext}}u &= u + K^*u, \end{aligned} \quad (28)$$

where a superscript int or ext denotes taking a limit from the interior or exterior of S , respectively. In general the formulas are true in the sense of non-tangential convergence almost everywhere on S (see [53]). These jump relations explain why the boundary condition (2) leads to the integral equation (5). In a moment we shall make a more precise statement about this. Before doing so, we need to show that the jump formulas hold in a certain trace sense.

For this purpose, we will also need to consider the Hilbert space $\mathcal{H}(V)/\mathbb{C}$ of harmonic functions v on V , modulo constants, with finite energy,

$$\|v\|_{\mathcal{H}(V)/\mathbb{C}}^2 = \int_V |\nabla v|^2 \, dr < \infty.$$

Since this semi-norm annihilates constants we consider v and $v + C$, $C \in \mathbb{C}$, to be the same element. Note that $\mathcal{H}(V)/\mathbb{C}$ is continuously contained in $H^1(V)/\mathbb{C}$ by the classical Poincaré inequality for V . Since V is assumed star-like, it is straightforward to use dilations in order to prove that functions which are harmonic and smooth in \overline{V} are dense in $H^1(V)/\mathbb{C}$. In fact, we introduced the hypothesis that V is star-like only to facilitate such density statements.

The Dirichlet problem

$$v \in \mathcal{H}(V)/\mathbb{C} \quad \text{Tr } v = u,$$

is well-posed for initial data $u \in H^{1/2}(S)$, see for example [14]. Equivalently, $\text{Tr} : \mathcal{H}(V)/\mathbb{C} \rightarrow H^{1/2}(S)/\mathbb{C}$ is a bicontinuous isomorphism. Often we will simply denote $\text{Tr } v = v|_S$ when it is clear what is meant.

It is established in a paper by Hofmann, Mitrea and Taylor [32] that Green's formula

$$\int_V \langle \nabla \phi, \nabla \psi \rangle \, dr + \int_V \phi \Delta \psi \, dr = \int_S \phi \partial_\nu \psi \, d\sigma \quad (29)$$

continues to hold true for S Lipschitz and $\phi, \psi \in C^\infty(\overline{V})$. Since the functions in $\mathcal{H}(V)/\mathbb{C}$ are harmonic, this shows that its scalar product satisfies

$$\langle v, w \rangle_{\mathcal{H}(V)/\mathbb{C}} = \int_V \langle \nabla v, \nabla \bar{w} \rangle \, dr = \int_S v \partial_\nu \bar{w} \, d\sigma = \int_S (\partial_\nu v) \bar{w} \, d\sigma.$$

Initially these identities are valid only for smooth v and w , but as in [35] one can argue by duality and density to interpret the normal derivatives

$\partial_\nu v$ and $\partial_\nu w$ as elements of $H^{-1/2}(S)$ so that the equalities remain true. If we denote by $H_0^{-1/2}(S)$ the closed subspace of those $u \in H^{-1/2}(S)$ such that $\int_S u \, d\sigma = 0$, the implied duality argument gives rise to a bicontinuous bijective operator $\partial_\nu : H^{1/2}(S)/\mathbb{C} \rightarrow H_0^{-1/2}(S)$ which should be understood as the normal derivative of the trace.

It is important for our purposes to now repeat this construction for the exterior space $\mathcal{H}(E)$ of harmonic functions v in E with finite energy norm and $\lim_{r \rightarrow \infty} v(r) = 0$. We state this as a proposition.

Proposition 4.1. *The exterior trace is a bicontinuous isomorphism when considered as an operator $\text{Tr}_E : \mathcal{H}(E) \rightarrow H^{1/2}(S)$. There is a corresponding bounded bijective operator $\partial_\nu^E : H^{1/2}(S) \rightarrow H^{-1/2}(S)$ satisfying*

$$\langle v, w \rangle_{\mathcal{H}(E)} = \int_E \langle \nabla v, \nabla \bar{w} \rangle \, dr = - \int_S v \partial_\nu^E \bar{w} \, d\sigma = - \int_S (\partial_\nu^E v) \bar{w} \, d\sigma.$$

Proof. The statements about Tr_E follow by the well-posedness of the Dirichlet problem, see [14]. The construction of ∂_ν^E again follows along the lines of [35]. \square

Remark 4.1. When $d = 2$ the additional condition $\int_S u \, d\sigma = 0$ is required to solve the exterior Dirichlet problem $v \in \mathcal{H}(E)$, $\text{Tr}_E v = u$. This is also reflected in the kernel $G(r, r')$ of the single layer potential. Note that $G(r, r') \sim -\frac{1}{2\pi} \log |r|$ as $r \rightarrow \infty$ for $d = 2$, but $\lim_{r \rightarrow \infty} G(r, r') = 0$ for $d > 2$.

We end this section with an interpretation of the jump relations (28) within the just established framework.

Proposition 4.2. *Let $u \in H^{1/2}(S)$, then $Du \in \mathcal{H}(V)/\mathbb{C}$, $Du \in \mathcal{H}(E)$ and*

$$\text{Tr } Du = -u + K^*u \quad \text{Tr}_E Du = u + K^*u.$$

Furthermore, let $v \in H^{-1/2}(S)$. Then $\mathcal{S}v \in \mathcal{H}(V)/\mathbb{C}$, $\mathcal{S}v \in \mathcal{H}(E)$ and

$$\text{Tr } \mathcal{S}v = \text{Tr}_E \mathcal{S}v = \mathcal{S}v|_S \quad \partial_\nu \mathcal{S}v = v + Kv \quad \partial_\nu^E \mathcal{S}v = -v + Kv.$$

Proof. Suppose first that u and v are smooth and harmonic on \overline{V} . Then by applying Green's formula we find that

$$Du(r) = \mathcal{S}(\partial_\nu u)(r) - 2u(r), \quad r \in V. \quad (30)$$

In particular, this shows that $Du|_V$ extends continuously to \overline{V} , and hence the jump relation $D^{\text{int}}u = -u + K^*u$ must hold in trace sense. That is, $\text{Tr } Du = -u + K^*u$. Since both sides of this equation are continuous maps of $H^{1/2}(S)$ by previously quoted results, it must hold for every $u \in H^{1/2}(S)$. By the same reasoning we obtain $\text{Tr } \mathcal{S}v = \mathcal{S}v|_S$ for every $v \in H^{-1/2}(S)$.

To show that $\partial_\nu \mathcal{S}v = v + Kv$ we note that $\mathcal{S}(\partial_\nu u) = u + K^*u$ by (30) and the jump formula. The sought formula is the dual statement of this. More precisely, for any smooth harmonic ψ we have

$$\begin{aligned}\langle \partial_\nu \mathcal{S}v, \psi \rangle_{L^2(S)} &= \langle \mathcal{S}v, \partial_\nu \psi \rangle_{L^2(S)} = \langle v, \mathcal{S}(\partial_\nu \psi) \rangle_{L^2(S)} \\ &= \langle v, \psi + K^* \psi \rangle_{L^2(S)} = \langle v + Kv, \psi \rangle_{L^2(S)},\end{aligned}$$

which verifies that $\partial_\nu \mathcal{S}v = v + Kv$ for all $v \in H^{-1/2}(S)$ by continuity and density.

The exterior statements are dealt with similarly. \square

5 Theory – results

5.1 Existence of the measure μ

We are now in a position to develop the symmetrization techniques that have been alluded to previously. Once these are in place, we can use the spectral theory of self-adjoint operators to prove that the (scaled) polarizability $\alpha(z) = \frac{\alpha(\epsilon_1, \epsilon_2)}{|V|\epsilon_1}$, $z = \frac{\epsilon_1 + \epsilon_2}{\epsilon_1 - \epsilon_2} \in \mathbb{C}$, has a representing measure μ .

We begin, however, by describing the sense in which the potential U will solve the boundary value problem given by (1), (2) and (3). Note that the following proposition furthermore expresses the fact that if looking for a potential such that $U(r) - e \cdot r$ has finite energy, then $H^{-1/2}(S)$ is exactly the right space to find the corresponding density distribution ρ .

Proposition 5.1. *Let $\rho \in H^{-1/2}(S)$ be such that (6) holds, i.e. $(K - z)\rho = g$, where $g(r) = -2(e \cdot \nu_r)$. Let*

$$U(r) = e \cdot r + \frac{1}{2} \mathcal{S}\rho(r), \quad r \in \mathbb{R}^d. \quad (31)$$

Then $U \in \mathcal{H}(V)/\mathbb{C}$, $U - e \cdot r \in \mathcal{H}(E)$, $\text{Tr } U = \text{Tr}_E U$, $\lim_{r \rightarrow \infty} \nabla U = e$ and U satisfies (2) in the sense that

$$\epsilon_1 (\partial_\nu^E(U - e \cdot r) + \partial_\nu(e \cdot r)) = \epsilon_2 \partial_\nu U. \quad (32)$$

The converse is also true. That is, if U satisfies the above properties, then there exists a $\rho \in H^{-1/2}(S)$ such that (31) and (6) hold.

Proof. This is a consequence of Proposition 4.2, the well-posedness of the interior and exterior Dirichlet problems and the bijectivity of $\mathcal{S} : H^{-1/2}(S) \rightarrow H^{1/2}(S)$. \square

Remark 5.1. When $z \neq -1$, the hypothesis that $(K - z)\rho = g$ implies that $\rho \in H_0^{-1/2}(S)$. This seen by taking into account that $g = -2\partial_\nu(e \cdot r)$ and $\partial_\nu \mathcal{S}\rho$ both belong to $H_0^{-1/2}(S)$ in the computation

$$z \int_S \rho \, d\sigma = \int_S K\rho - g \, d\sigma = \int_S K\rho \, d\sigma = \int_S \partial_\nu \mathcal{S}\rho - \rho \, d\sigma = - \int_S \rho \, d\sigma.$$

This is of importance for the case $d = 2$ (cf. Remark 4.1).

In the sequel we shall denote $\rho = \rho_z$ and $U = U_z$ to indicate their dependence on z . Under the hypothesis of the preceding proposition, we can, due to the assumption of isotropy, express the scaled polarizability as

$$\begin{aligned}\alpha(z) &= \frac{\epsilon_2 - \epsilon_1}{|V|\epsilon_1} \int_V \nabla U_z(r) \cdot e \, dr = \frac{\epsilon_2 - \epsilon_1}{|V|\epsilon_1} \int_S (\partial_\nu U_z)(r) (e \cdot r) \, d\sigma_r \\ &= \frac{\epsilon_2 - \epsilon_1}{|V|\epsilon_1} \int_S (e \cdot \nu_r + \frac{1}{2}(\rho_z + K\rho_z)(r)) (e \cdot r) \, d\sigma_r \\ &= \frac{\epsilon_2 - \epsilon_1}{|V|\epsilon_1} \frac{z + 1}{2} \int_S \rho_z(r) (e \cdot r) \, d\sigma_r = \int_S \rho_z h \, d\sigma,\end{aligned}$$

where $h(r) = -(e \cdot r)/|V|$. Since $(K - z)\rho_z = g$, this shows that the analysis of α is closely related to the spectral theory of K .

The scalar product on $\mathcal{H}(V)/\mathbb{C}$ is one of the keys to understanding the spectral theory of K and K^* , since K^* is self-adjoint in the $\mathcal{H}(V)/\mathbb{C}$ -pairing. To be precise, the above shows that any element $v \in H^{1/2}(S)/\mathbb{C}$ can also be considered as an element $v \in \mathcal{H}(V)/\mathbb{C}$ in a bicontinuous way. We are therefore justified in letting $H^{1/2}(S)/\mathbb{C}$ inherit its scalar product from $\mathcal{H}(V)/\mathbb{C}$,

$$\langle v, w \rangle_{H^{1/2}(S)/\mathbb{C}} = \langle v, w \rangle_{\mathcal{H}(V)/\mathbb{C}}.$$

Since K^* maps constants onto constants (cf. (30)), we may consider K^* as a bounded map on $H^{1/2}(S)/\mathbb{C}$. Let $v, w \in H^{1/2}(S)/\mathbb{C}$. By the fact that $K^*v = \mathcal{S}(\partial_\nu v) - v$ it then holds that

$$\begin{aligned}\langle K^*v, w \rangle_{H^{1/2}(S)/\mathbb{C}} &= \int_S ((\mathcal{S}(\partial_\nu v) - v)(\partial_\nu \bar{w})) \, d\sigma \\ &= \int_S v \partial_\nu (\mathcal{S}(\partial_\nu \bar{w}) - \bar{w}) \, d\sigma = \langle v, K^*w \rangle_{H^{1/2}(S)/\mathbb{C}}.\end{aligned}$$

Theorem 5.2. *There exists a compact set $L \subset \mathbb{R}$ and a positive Borel measure μ with total mass 2 and compact support contained in L , such that for $z \in \mathbb{C}$, $z \notin L$, $(K - z)\rho = g$ has a unique solution $\rho_z \in H_0^{-1/2}(S)$ and*

$$\alpha(z) = \int_{\mathbb{R}} \frac{d\mu(x)}{x - z}. \quad (33)$$

μ is unique in the class of compactly supported finite Borel measures such that (33) holds for all $z \in \mathbb{C}_+ = \{z : \Im z > 0\}$.

Proof. Since K^* is bounded and self-adjoint on $H^{1/2}(S)/\mathbb{C}$ it has by the spectral theorem a corresponding projection-valued spectral measure \mathcal{E} with support in the spectrum of K^* . Let $L = \text{Spec } K^*$. \mathcal{E} is characterized by the fact that for every bounded Borel-measurable function f on L , it holds that

$$f(K^*) = \int_L f(x) \, d\mathcal{E}(x). \quad (34)$$

For any $z \notin L$ note that $K^* - \bar{z}$ is invertible on $H^{1/2}(S)/\mathbb{C}$, and hence $K - z$ is invertible on the dual space $H_0^{-1/2}(S)$. Since $h \in H^{1/2}(S)$ and $g = 2|V|\partial_\nu h \in H_0^{-1/2}(S)$ we have

$$\begin{aligned}\alpha(z) &= \langle (K - z)^{-1}g, h \rangle_{L^2(S)} = \langle g, (K^* - \bar{z})^{-1}h \rangle_{L^2(S)} \\ &= 2|V|\langle \partial_\nu h, (K^* - \bar{z})^{-1}h \rangle_{L^2(S)} = 2|V|\langle h, (K^* - \bar{z})^{-1}h \rangle_{H^{1/2}(S)/\mathbb{C}} \\ &= 2|V|\langle (K^* - z)^{-1}h, h \rangle_{H^{1/2}(S)/\mathbb{C}}.\end{aligned}$$

With $\mu(R) = 2|V|\langle \mathcal{E}(R)h, h \rangle_{H^{1/2}(S)/\mathbb{C}}$ for any Borel set $R \subset \mathbb{R}$ we obtain by applying (34) with $f(x) = 1/(x - z)$ the desired formula

$$\alpha(z) = \int_{\mathbb{R}} \frac{d\mu(x)}{x - z}.$$

The constructed measure μ is positive since $\mu(R) = 2|V|\langle \mathcal{E}(R)h, h \rangle = 2|V|\langle \mathcal{E}(R)h, \mathcal{E}(R)h \rangle = 2|V|\|\mathcal{E}(R)h\|^2 \geq 0$, and since $\mathcal{E}(\mathbb{R})$ is the identity operator, its total mass is

$$\|\mu\| = 2|V|\|h\|^2 = 2\frac{1}{|V|} \int_V |e|^2 dr = 2.$$

Equation (33) expresses that α is the Cauchy transform of μ , $\alpha(z) = \mathcal{K}_\mu(z)$. See Cima, Matheson and Ross [8] for an excellent survey of the Cauchy transform, written for measures with support on the unit circle, but all results can be transformed to results about measures on \mathbb{R} through standard conformal mapping techniques. See Koosis [37] for an explanation of this latter point, as well as results stated directly for the real line. By the classical F. and M. Riesz theorem, any other measure μ^* supported on \mathbb{R} and such that $\mathcal{K}_{\mu^*}(z) = \alpha(z) = \mathcal{K}_\mu(z)$ for $z \in \mathbb{C}_+$ must be of the form $d\mu^* = d\mu + \bar{u} dx$, where $u \in \mathcal{H}^1(\mathbb{C}_+)$ is given by the boundary values of an analytic Hardy space-function in the upper half-plane. Since such a function u can never be compactly supported unless it is identically zero, we obtain the uniqueness part of the theorem. \square

Remark 5.2. The fact that $\|\mu\| = 2$ is sum rule (22). Note also that $L = \text{Spec}(K^*, H^{1/2}/\mathbb{C}) = \text{Spec}(K, H_0^{-1/2})$ only differs from $\text{Spec}(K^*, H^{1/2}) = \text{Spec}(K, H^{-1/2})$ by the point $z = -1$, which is in the latter spectrum but not in the former (see [44]).

The considerations leading up to the previous theorem are quite similar in spirit to those of Bergman [2]. Bergman considers a different potential operator which is symmetric under the inner product $\int_V \langle \nabla v, \nabla w \rangle dr$, although the arguments presented are somewhat incomplete since a space of functions belonging to this inner product is not identified.

Before discussing the specific features of α and μ we shall investigate a different symmetrization approach, expounded upon in the case when S is

a C^2 -surface by Khavinson, Putinar and Shapiro [35]. The starting point is Plemelj's symmetrization principle, which says that $\mathcal{S}K = K^*\mathcal{S}$ on $L^2(S)$ and continues to hold true in our situation with the same proof as in [35]. This operator equality amounts to the statement that K is self-adjoint under the inner product $\langle \mathcal{S}u, v \rangle_{L^2(S)}$. Note that \mathcal{S} is a strictly positive operator on $L^2(S)$, so that the form $(u, v) \rightarrow \langle \mathcal{S}u, v \rangle_{L^2(S)}$ is strictly positive definite. The advantage this form has over $\langle \partial_\nu u, v \rangle_{L^2(S)}$ lies in the fact that \mathcal{S} is a bounded (even compact) map on $L^2(S)$, while ∂_ν is not. This will allow us to gain some further insight into the structure of K and K^* .

Instead of working with the completion of $L^2(S)$ under $\langle \mathcal{S}u, u \rangle_{L^2(S)}$, we shall follow the approach of [35] and introduce an operator-theoretic formalism to express the symmetrization of K . Recall that $K : L^2(S) \rightarrow L^2(S)$ is compact when S is C^2 , and so its spectrum consists of the point 0 and a sequence (z_i) of non-zero eigenvalues tending to zero, every eigenspace $H_z(K) = \ker(K - z)$ having finite dimension when $z \neq 0$.

Theorem 5.3 ([35]). *Suppose that S is a C^2 -surface. Then there exists a self-adjoint compact operator $A : L^2(S) \rightarrow L^2(S)$ such that $A\sqrt{\mathcal{S}} = \sqrt{\mathcal{S}}K$ on $L^2(S)$. When $z \neq 0$, $\sqrt{\mathcal{S}} : H_z(K) \rightarrow H_z(A)$ and $\sqrt{\mathcal{S}} : H_z(A) \rightarrow H_z(K^*)$ are isomorphisms of the indicated eigenspaces, and the eigenvectors of K^* (including those for $z = 0$) span $L^2(S)$. In particular, the $L^2(S)$ -spectrum of K^* is real.*

From the point of view of Khavinson et al., the proof of this theorem parallels the symmetrization theory of Krein [38]. However, a result about operator equations due to Douglas [12] essentially assures us of the existence of A even when K is only bounded, that is, when S is only Lipschitz. See Hassi, Sebestyén and de Snoo [23] for a precise proof. The key fact is still that $\mathcal{S}K = K^*\mathcal{S}$.

Proposition 5.4. *There exists a bounded self-adjoint operator $A : L^2(S) \rightarrow L^2(S)$ such that $A\sqrt{\mathcal{S}} = \sqrt{\mathcal{S}}K$ on $L^2(S)$.*

Proof. Given the existence of a bounded operator A on $L^2(S)$ satisfying $A\sqrt{\mathcal{S}} = \sqrt{\mathcal{S}}K$, we deduce from the equation $\sqrt{\mathcal{S}}A\sqrt{\mathcal{S}} = \mathcal{S}K = K^*\mathcal{S} = \sqrt{\mathcal{S}}A^*\sqrt{\mathcal{S}}$, and the injectivity and dense range of \mathcal{S} , that A must in fact be self-adjoint. \square

We also require the following result contained in [35, Proposition 1], with a proof that carries over to our setting.

Proposition 5.5. *$\sqrt{\mathcal{S}} : L^2(S) \rightarrow H^{1/2}(S)$ is a bicontinuous isomorphism. Dually, $\sqrt{\mathcal{S}}$ also extends to a bicontinuous isomorphism $\sqrt{\mathcal{S}} : H^{-1/2}(S) \rightarrow L^2(S)$.*

The existence of A gives us another way to derive the existence of a measure μ such that $\alpha(z) = \int_{\mathbb{R}} \frac{d\mu(x)}{x-z}$. Since

$$(K - z)^{-1} = \sqrt{\mathcal{S}}^{-1}(A - z)^{-1}\sqrt{\mathcal{S}} \quad (35)$$

as an inverse on $H^{-1/2}(S)$, we can write

$$\alpha(z) = \langle (K - z)^{-1}g, h \rangle_{L^2(S)} = \langle (A - z)^{-1}\sqrt{\mathcal{S}}g, \sqrt{\mathcal{S}}^{-1}h \rangle_{L^2(S)},$$

where, clearly, $\sqrt{\mathcal{S}}g, \sqrt{\mathcal{S}}^{-1}h \in L^2(S)$. If \mathcal{E}_A is the spectral measure of A , we therefore obtain a measure with the desired property by letting $\mu(R) = \langle \mathcal{E}_A(R)\sqrt{\mathcal{S}}g, \sqrt{\mathcal{S}}^{-1}h \rangle_{L^2(S)}$ for $R \subset \mathbb{R}$. In this way we recover all the conclusions of Theorem 5.2 except for the positivity of μ . The positivity appears, to the authors, to be elusive when working with this second symmetrization technique.

5.2 Properties of the polarizability $\alpha(z)$ and the measure μ

In the final part of this section we will employ all the tools introduced thus far, in order to understand the behavior and specific features of the polarizability $\alpha(z)$ and its related measure μ . We begin by discussing the case of a smooth surface S , giving a rigorous treatment of many of the formulas and ideas that appear in the paper [40] by Mayergoyz, Fredkin and Zhang. From there we discuss the idea of approximating a non-smooth surface by a sequence of smooth surfaces, proving that the corresponding representing measures converge in a weak-star sense. We conclude with an analysis of the measure μ in the general non-smooth case, in particular giving a condition which guarantees that it does not have a singular part. Furthermore, we show that even though the polarizability $\alpha^+(x)$ exists in a limit sense almost everywhere $x \in \mathbb{R}$, the potential U_x does not exist at points where $\mu'(x) > 0$, neither as a solution of the boundary value problem given by (1), (2) and (3), nor in a limit sense.

Suppose now that S is a C^2 -surface, so that the operator A is compact. Let (f_i^0) be an orthonormal basis for $\ker A$, and let (f_i^1) be eigenvectors of A corresponding to the non-zero eigenvalues (z_i^1) , repeated according to multiplicity, so that $(f_i) = (f_i^0) \cup (f_i^1)$ is an orthonormal basis for $L^2(S)$. By Theorem 5.3, $K, K^* : L^2(S) \rightarrow L^2(S)$ have the same non-zero eigenvalues (z_i^1) , and corresponding (non-orthonormal) eigenvectors are obtained as $\phi_i^1 = \sqrt{\mathcal{S}}^{-1}f_i^1$ and $\psi_i^1 = \sqrt{\mathcal{S}}f_i^1$, respectively. Concerning zero eigenvectors, $\psi_i^0 = \sqrt{\mathcal{S}}f_i^0 \in H^{1/2}(S)$ are clearly in the kernel of K^* , but $\phi_i^0 = \sqrt{\mathcal{S}}^{-1}f_i^0$ are in general elements of $H^{-1/2}(S)$ and only zero eigenvectors of K when considered as an operator on said space $H^{-1/2}(S)$. In particular, we note that the $H^{-1/2}(S)$ -eigenvectors of K span the whole space $H^{-1/2}(S)$. With

this in mind, we shall denote $(\phi_i) = (\phi_i^0) \cup (\phi_i^1)$ and $(\psi_i) = (\psi_i^0) \cup (\psi_i^1)$, the indexing arranged appropriately so that

$$\langle \phi_i, \psi_j \rangle_{L^2(S)} = \delta_{ij}.$$

As a final notational detail, we shall let (z_i) denote the full sequence of eigenvalues including zeros, so that $K\phi_i = z_i\phi_i$ and $K^*\psi_i = z_i\psi_i$ for every i .

Based on the spectral decomposition of A we obtain for $u \in L^2(S)$ that

$$\sqrt{S}Ku = A\sqrt{S}u = \sum_i z_i \langle \sqrt{S}u, f_i \rangle_{L^2(S)} f_i,$$

with convergence in $L^2(S)$. Equivalently, we have for $u \in H^{-1/2}(S)$ the expansion

$$Ku = \sum_i z_i \langle u, \psi_i \rangle_{L^2(S)} \phi_i, \quad (36)$$

with convergence in $H^{-1/2}(S)$. This is the formal interpretation of equation (12). In this framework it is now easy to furthermore justify the formulas (17), (18) and (19). We state this as a theorem.

Theorem 5.6. *Let S be a C^2 -surface. Then (36) holds with K considered as an operator on $H^{-1/2}(S)$. Furthermore, let $u_i = \langle \phi_i, h \rangle_{L^2(S)}$ and $v_i = \langle g, \psi_i \rangle_{L^2(S)}$. Then*

$$\text{Spec}(K, L^2(S)) = \text{Spec}(K, H^{-1/2}(S)) = \{(z_i)\}, \quad (37)$$

and for $z \notin (z_i)$ the unique solution $\rho_z \in L^2(S)$ of $(K - z)\rho = g$ is given by

$$\rho_z = \sum_i \frac{v_i \phi_i}{z_i - z}, \quad (38)$$

with convergence in $H^{-1/2}(S)$. The corresponding formula for the scaled polarizability is

$$\alpha(z) = \sum_i \frac{u_i v_i}{z_i - z}, \quad (39)$$

where the sum is absolutely convergent. Finally, it holds that $\sum_i u_i v_i = 2$.

Proof. Equation (35) and Theorem 5.3 show that

$$\text{Spec}(K, H^{-1/2}(S)) = \text{Spec}(A, L^2(S)) = \text{Spec}(K, L^2(S)).$$

Formula (38) also follows from (35) and spectral decomposition of A , since

$$\rho_z = \sqrt{S}^{-1}(A - z)^{-1}\sqrt{S}g = \sqrt{S}^{-1} \sum_i \frac{\langle \sqrt{S}g, f_i \rangle_{L^2(S)} f_i}{z_i - z} = \sum_i \frac{v_i \phi_i}{z_i - z}.$$

From $\alpha(z) = \langle \rho_z, h \rangle_{L^2(S)}$ we now deduce (39). In terms of the measure μ , this expresses the fact that $\mu = \sum_i u_i v_i \delta_{z_i}$ where δ_{z_i} is the Dirac delta at z_i . This makes it clear that we have already proven that $\sum_i u_i v_i = 2$ as a part of Theorem 5.2. \square

Remark 5.3. The statement that the $H^{-1/2}(S)$ -spectrum of K is equal to its $L^2(S)$ -spectrum is markedly untrue when S is not C^2 . In fact, when S is a square in two dimensions the $H^{-1/2}(S)$ -spectrum of K is real, while the $L^2(S)$ -spectrum extends into the complex plane.

We will now briefly discuss the limiting process which occurs when (S_k) is a sequence of smooth surfaces approximating a non-smooth surface S . For brevity we assume that S is the cube defined by $\max_{1 \leq i \leq d} |r_i| = 1$ in d dimensions, $r = (r_1, \dots, r_d)$, and that S_k is the superellipsoid defined by $\sum_{i=1}^d |r_i|^k = 1$. We shall also skip some rather laborious details. See [53] for detailed approximation arguments when S is a general Lipschitz surface.

For any notation introduced so far, we denote by a subscript k that it corresponds to the surface S_k rather than S . Via appropriately defined homeomorphisms of S_k onto S we may, in a bicontinuous way, consider K_k^* and K^* to be operators on the same space $H^{1/2}(S)$. We choose the implied isomorphism between $H^{1/2}(S)$ and $H^{1/2}(S_k)$ so that it extends to a unitary map of $L^2(S)$ onto $L^2(S_k)$. Similar conventions will apply throughout what follows. Using the boundedness results collected in Section 4 and adapting the arguments in the proof of [53, Theorem 3.1], one can verify that K_k^* converges strongly to K^* on $H^{1/2}(S)$, meaning that $\lim_k K_k^* u = K^* u$ in norm for any $u \in H^{1/2}(S)$. Similarly, K_k converges strongly to K on $H^{-1/2}(S)$.

We can use the spectral representations (34) of K^* and K_k^* to find that any $z \in \text{Spec}(K^*, H^{1/2}) = \text{Spec}(K, H^{-1/2})$ is obtained as the limit of a sequence of eigenvalues $z_k \in \text{Spec}(K_k^*, H^{1/2}) = \text{Spec}(K_k, H^{-1/2})$ (see Weidmann [55]). From (27) and (37) we deduce that

$$\text{Spec}(K^*, H^{1/2}(S)) \subset [-1, 1].$$

However, unlike the case of convergence in operator norm, we point out that strong convergence allows us to say very little about the character of the points in $\text{Spec}(K^*, H^{1/2})$. For example, they do not need to be eigenvalues.

Let $z \in \mathbb{C}$ be a point at a distance at least $\varepsilon > 0$ away from the $H^{-1/2}(S)$ -spectra of K and K_k , for all k . It is evident from (38) that $\sup_k \|\rho_{z,k}\|_{H^{-1/2}(S)} < \infty$. We can hence extract a weakly convergent subsequence $\rho_{z,k'}$ with limit b ,

$$\lim_{k' \rightarrow \infty} \langle \rho_{z,k'}, w \rangle_{L^2(S)} = \langle b, w \rangle_{L^2(S)}, \quad \forall w \in H^{1/2}(S).$$

Since $s\text{-}\lim K_k = K$ we find that $(K_{k'} - z)\rho_{z,k'}$ converges weakly to $(K - z)b$. On the other hand, $(K_{k'} - z)\rho_{z,k'} = g_{k'}$ converges to g . Hence $b = \rho_z$.

Since every weakly convergent subsequence of $\rho_{z,k}$ has the same limit ρ_z , we conclude that $\rho_{z,k}$ converges weakly to ρ_z . In particular, noting that $h_k \rightarrow h$ in $H^{1/2}(S)$,

$$\lim_{k \rightarrow \infty} \alpha_k(z) = \lim_{k \rightarrow \infty} \langle \rho_{z,k}, h_k \rangle_{L^2(S)} = \alpha(z).$$

We summarize.

Theorem 5.7. *Let S be the unit cube in \mathbb{R}^d , and let S_k be the approximating superellipsoid given by $\sum_{i=1}^d |r_i|^k = 1$, $r = (r_1, \dots, r_d)$. Denoting by $\text{cl } R$ the closure of $R \subset \mathbb{R}$, let*

$$B = \text{cl} \left[\bigcup_k \text{Spec}(K_k, H^{-1/2}(S_k)) \right].$$

Then $\text{Spec}(K, H^{-1/2}(S)) \subset B \subset [-1, 1]$ and $\lim_k \alpha_k(z) = \alpha(z)$ for all $z \notin B$. Furthermore, the supports of μ_k and μ are contained in B , and μ_k converges weak-star to μ as measures on B . That is,

$$\lim_{k \rightarrow \infty} \int_{\mathbb{R}} f(x) d\mu_k(x) = \int_{\mathbb{R}} f(x) d\mu(x), \quad \forall f \in C(B), \quad (40)$$

where $C(B)$ denotes the continuous functions on B .

Proof. Only the final point remains to be proven. However, the argument immediately preceding the theorem can be repeated to show that (40) holds for $f(x) = 1/(x - z)^t$, where $z \notin B$ and $t \geq 0$ is an integer. Now (40) immediately follows in general from the fact that the linear span of such functions $1/(x - z)^t$ is dense in $C(B)$, which in turn follows for example from the Stone-Weierstrass theorem. \square

We turn to the discussion of μ and α for a general Lipschitz surface S . First note that the support of μ is contained in the $H^{-1/2}(S)$ -spectrum of K , and that μ has a unique decomposition

$$\mu = \mu_a + \mu_p + \mu_s.$$

Here μ_a is the absolutely continuous part of the measure, so that $\mu_a = \mu'(x) dx$, where $\mu' \in L^1(\mathbb{R})$. μ has at most a countable number of atoms z_i , corresponding to bright plasmons at z_i , and μ_p is the atomic part of μ ,

$$\mu_p = \sum_i \mu(\{z_i\}) \delta_{z_i}.$$

Note that each atom arises from an eigenvalue z of K , but not necessarily every eigenvalue is given positive measure by μ , reflecting the distinction between bright and dark plasmons. Finally, μ_s denotes the singular part of μ , excluding atoms. This means that μ_s has no atoms, yet lives solely on a

set with Lebesgue measure zero. That is, there exists a measure zero set R_0 such that $\mu_s(R) = 0$ for any Borel set $R \subset \mathbb{R}$ with $R \cap R_0 = \emptyset$.

For $0 < p < \infty$, let $\mathcal{H}_{\text{conf}}^p(\mathbb{C}_+)$ denote the conformally invariant Hardy space on the upper half-plane \mathbb{C}_+ , consisting of analytic functions f in \mathbb{C}_+ such that

$$\|f\|_p^p = \sup_{r>0} \int_{y=r} \frac{|f(z)|^p}{|z+i|^2} dx < \infty, \quad z = x + iy.$$

This is known as the conformally invariant Hardy space as

$$\mathcal{H}_{\text{conf}}^p(\mathbb{C}_+) = \{f \circ \omega : f \in H^p(\mathbb{D})\},$$

where $H^p(\mathbb{D})$ is the usual Hardy space of the unit disk and ω is a conformal map of \mathbb{C}_+ onto the disk. $\mathcal{H}_{\text{conf}}^p(\mathbb{C}_+)$ does not coincide with the usual Hardy space of the upper half-plane. Of importance to us is the fact that every $f \in \mathcal{H}_{\text{conf}}^p(\mathbb{C}_+)$ has boundary values $f(x) = \lim_{y \rightarrow 0^+} f(x+iy)$ almost everywhere, and

$$\|f\|_p^p = \int_{\mathbb{R}} \frac{|f(x)|^p}{1+x^2} dx.$$

See Koosis [37] for further information.

As previously mentioned in the proof of Theorem 5.2, α is the Cauchy transform of μ , $\alpha(z) = \mathcal{K}_\mu(z)$. Changing variables in the Cauchy transform through ω , exploiting that μ is compactly supported and applying Smirnov's theorem (see [8]) leads to the fact that $\alpha \in \mathcal{H}_{\text{conf}}^p(\mathbb{C}_+)$ for $0 < p < 1$. Hence, α has boundary values $\alpha^+(x)$ for almost all $x \in \mathbb{R}$, taken as limits from the upper half-plane. A similar discussion could be carried out for the lower half-plane, but since μ is real, the boundary values obtained from below are related to those obtained from above simply by conjugation.

The absolutely continuous part of μ is related to α^+ through equation (25) almost everywhere, $\pi\mu'(x) = \Im(\alpha^+(x))$. Atoms z_i can be recognized as those points where $|\alpha(z_i + i\varepsilon)| \sim \varepsilon^{-1}$ as $\varepsilon \rightarrow 0^+$. While some results are available, see [8], recovering μ_s from α is much more subtle. However, if it turns out to be the case that

$$\int_{\mathbb{R}} \frac{|\alpha^+(x)|}{1+x^2} dx < \infty, \quad (41)$$

it follows that $\alpha \in \mathcal{H}_{\text{conf}}^1(\mathbb{C}_+)$. But then $f \circ \omega^{-1}$ is the Cauchy integral of its boundary values and we infer that μ must be absolutely continuous. That is, in this case $\mu_p = \mu_s = 0$ and

$$\alpha(z) = \int_{\mathbb{R}} \frac{\mu'(x) dx}{x-z}, \quad z \notin \text{Spec}(K, H_0^{-1/2}(S)). \quad (42)$$

While we offer no strict proof, the numerical evidence in Sections 10 and 11 suggests that (41) holds when S is a square in two dimensions or a cube in three, and hence that (42) holds.

To end this section we shall show that while $\alpha(z)$ has boundary values $\alpha^+(x)$ almost everywhere, the same cannot be said of the corresponding solutions ρ_z . Note that the limit $\lim_{h \rightarrow 0} \int_x^{x+h} d\mu$ exists finitely almost everywhere for $x \in \mathbb{R}$. We say that $\mu'(x)$ exists whenever this is so,

$$\mu'(x) = \lim_{h \rightarrow 0} \int_x^{x+h} d\mu,$$

and as before we denote by σ_μ the set

$$\sigma_\mu = \{x \in \mathbb{R} : \mu'(x) > 0 \text{ exists}\}.$$

Theorem 5.8. *For $x \in \mathbb{R}$ and $\varepsilon > 0$, let $\rho_{x+i\varepsilon} \in H^{-1/2}(S)$ denote the unique solution of $(K - x - i\varepsilon)\rho_{x+i\varepsilon} = g$. For any $x \in \sigma_\mu$, we have*

$$\lim_{\varepsilon \rightarrow 0^+} \|\rho_{x+i\varepsilon}\|_{H^{-1/2}(S)} = \infty, \quad (43)$$

and moreover, the equation $(K - x)\rho = g$ has no solution $\rho \in H^{-1/2}(S)$. Hence, for such x , there exists no potential U_x solving the boundary value problem (1), (2), (3) in the sense given by Proposition 5.1.

Proof. If (43) does not hold, there is a sequence (ε_n) with $\varepsilon_n \rightarrow 0$ as $n \rightarrow \infty$ and such that $\lim_{n \rightarrow \infty} \rho_{x+i\varepsilon_n}$ exists weakly. From the proof of Theorem 5.2 we see that $\tau_{x+i\varepsilon_n} = (K^* - x - i\varepsilon_n)^{-1}h$ converges weakly in $H^{1/2}(S)/\mathbb{C}$ to some element τ_x , meaning that

$$\lim_{n \rightarrow \infty} \langle \tau_{x+i\varepsilon_n}, w \rangle_{H^{1/2}(S)/\mathbb{C}} = \langle \tau_x, w \rangle_{H^{1/2}(S)/\mathbb{C}}, \quad \forall w \in H^{1/2}(S)/\mathbb{C}.$$

Then, clearly, it must be that

$$(K^* - x)\tau_x = h. \quad (44)$$

Let μ_{τ_x} be the positive measure defined by $\mu_{\tau_x}(t) = \langle \mathcal{E}(t)\tau_x, \tau_x \rangle_{H^{1/2}(S)/\mathbb{C}}$, where \mathcal{E} is the spectral measure of K^* on $H^{1/2}(S)/\mathbb{C}$. Recalling that $\mu(t) = 2|V|\langle \mathcal{E}(t)h, h \rangle_{H^{1/2}(S)/\mathbb{C}}$, we can reformulate (44) as

$$\mu(t) = 2|V|(t - x)^2 \mu_{\tau_x}(t).$$

We infer

$$\int_{\mathbb{R}} \frac{d\mu(t)}{(t - x)^2} < \infty.$$

This implies that $\lim_{y \rightarrow 0^+} P_\mu(x + iy) = 0$ for the Poisson integral

$$P_\mu(z) = \frac{1}{\pi} \int_{\mathbb{R}} \frac{y d\mu(t)}{(t - x)^2 + y^2}, \quad z = x + iy \in \mathbb{C}_+.$$

On the other hand, it is well known that $\lim_{y \rightarrow 0^+} P_\mu(x + iy) = \mu'(x)$ whenever the right hand side exists finitely. This contradicts the hypothesis that $\mu'(x) \neq 0$.

Suppose that there exists a $\rho \in H^{-1/2}(S)$ such that $(K - x)\rho = g$. Note that

$$(A - x - i\varepsilon)^{-1}(A - x) = \int_{\mathbb{R}} \frac{t - x}{t - x - i\varepsilon} d\mathcal{E}_A(t),$$

where \mathcal{E}_A is the spectral measure of A on $L^2(S)$. Hence the operator norms $\|(A - x - i\varepsilon)^{-1}(A - x)\|$ are uniformly bounded for $\varepsilon > 0$. Since

$$\rho_{x+i\varepsilon} = (K - x - i\varepsilon)^{-1}(K - x)\rho = \sqrt{\mathcal{S}}^{-1}(A - x - i\varepsilon)^{-1}(A - x)\sqrt{\mathcal{S}}\rho$$

we have obtained a contradiction to (43). \square

Remark 5.4. As to be expected, a similar argument shows that the conclusions of Theorem 5.8 are valid also when $x \in \mathbb{R}$ is such that $\mu(\{x\}) > 0$, that is, when there is a bright plasmon at x .

6 Capacitance

The electrical capacitance C of an isolated charged conducting body V can be defined as the ratio of its total charge to its constant potential $U(r)$. The problem of calculating C for V being a (unit) cube has “long been considered one of the major unsolved problems of electrostatic theory” [49] and attracted interest by researchers in computational electromagnetics for half a century. See [3, 33, 46] for recent contributions along with reviews of previous work and tables of historical progress. The highest relative precision for C so far, 10^{-7} , was achieved in 2010 by parallelizing a Monte Carlo method and running it on a PC cluster [33]. See also Table 1.

The problem of determining C can be modeled as an integral equation much in the same way as the problem of determining $\alpha(z)$ and we omit details. If one solves

$$(I + K + Q)\rho(r) = 1, \quad (45)$$

where K is as in (10) and Q is the surface integral operator

$$Q\rho = \int_S \rho(r) d\sigma_r, \quad (46)$$

then the (normalized) capacitance can be evaluated as

$$C = \frac{1}{4\pi U(r)}, \quad r \in V, \quad (47)$$

where

$$U(r) = \int_S G(r, r')\rho(r') d\sigma_{r'}. \quad (48)$$

7 Strategies for computing $\alpha^+(x)$

The difficulties with computing $\alpha^+(x)$ when S has edges and corners relate to issues of stability and resolution. We know from Theorem 5.8 that the electrostatic problem does not have a finite energy solution $U(r)$ and that (6) does not have a solution $\rho(r) \in H^{-1/2}(S)$ for $z \in \sigma_\mu$. Close to σ_μ , stability problems can be expected. A computational mesh needs to be extremely refined (locally) in order to resolve $U(r)$ or $\rho(r)$ and the solver must have the capability of dealing with strongly singular solutions.

One strategy for alleviating these problems is to round edges and corners so that S becomes smooth. Then $U(r)$ has finite energy and $\rho(r) \in L^2(S)$, except for at $z = z_i$, and $\alpha(z)$ assumes the form (18). Some distance above the real axis, corresponding to bigger losses, $\alpha(z)$ may resemble $\alpha^+(x)$ and can be evaluated using commercial software. This is essentially the approach in [34, 54, 56], where finite element solvers are chosen.

It is, however, possible and advantageous to take the limit $z \rightarrow \sigma_\mu$ in $\alpha(z)$ numerically while letting S retain its sharp shape. The rounding of edges and corners, while smoothing solutions, introduces new length-scales which is an unnecessary complication. In fact, there has been an intense activity in the area of constructing numerical algorithms for solving integral equations on non-smooth curves in recent years [4, 5, 6, 7, 25, 26, 29, 30]. See [27, Section 1.3] for an overview and a comparison of various approaches. Sharp corners and other boundary singularities can be treated extremely efficiently using fast direct and fully automatic solvers and by taking advantage of asymptotic self-similarity. An algorithm to this effect for a quantity analogous to $\alpha(z)$ for squares in a periodic setting is assembled in [27] and tested thoroughly in [28]. This paper continues along the lines of that work.

8 Algorithm for the square

This section is a summary of results from Refs. [25, 27] applied to the solution of (10) for V being a square. We construct two meshes on S – a coarse mesh and a fine mesh. The coarse mesh has 16 quadrature panels. The fine mesh is constructed from the coarse mesh by n_{sub} times subdividing the panels closest to each corner vertex s_k in a direction towards the vertex. See Fig. 1.

8.1 Preconditioning and discretization

Let S_k^* denote a segment of S covering the four panels on the coarse mesh that lie closest to the corner vertex s_k – two panels on each side of s_k . The S_k^* are disjoint and their union is S . Let $K(r, r')$ denote the kernel of K in (10). Split $K(r, r')$ into two functions

$$K(r, r') = K^*(r, r') + K^\circ(r, r'), \quad (49)$$

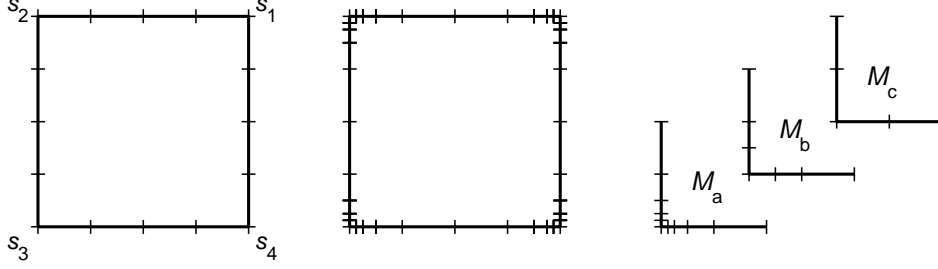


Figure 1: Meshes on the boundary S of a square. Left: the coarse mesh and the corner vertices s_k . Middle: a mesh that is refined $n_{\text{sub}} = 3$ times. Right: local meshes \mathcal{M}_a , \mathcal{M}_b and \mathcal{M}_c centered around the corner vertex s_3 .

where $K^*(r, r')$ is zero except for when r and r' simultaneously lie on the same S_k^* . In this latter case $K^\circ(r, r')$ is zero.

The kernel split (49) corresponds to an operator split $K = K^* + K^\circ$ where K° is a compact operator. Discretization of (10), using a Nyström method based on composite 16-point Gauss–Legendre quadrature and a coarse or a fine mesh on S , leads to an equation of the form

$$(\mathbf{I} + \lambda \mathbf{K}^* + \lambda \mathbf{K}^\circ) \boldsymbol{\rho} = \lambda \mathbf{g}, \quad (50)$$

where \mathbf{I} , \mathbf{K}^* , and \mathbf{K}° are square matrices and $\boldsymbol{\rho}$ and \mathbf{g} are columns vectors. The matrix \mathbf{K}^* assumes a block-diagonal structure since the S_k^* are disjoint. This will be important in what follows.

The change of variables

$$\rho(r) = (I + \lambda K^*)^{-1} \tilde{\rho}(r) \quad (51)$$

makes (50) read

$$\left(\mathbf{I} + \lambda \mathbf{K}^\circ (\mathbf{I} + \lambda \mathbf{K}^*)^{-1} \right) \tilde{\boldsymbol{\rho}} = \lambda \mathbf{g}. \quad (52)$$

This right preconditioned equation corresponds to the discretization of a Fredholm second kind equation with a composed compact operator. The solution $\tilde{\boldsymbol{\rho}}$ is the discretization of a function that is piecewise smooth and can be resolved by piecewise polynomials.

From now on we let subscripts fin and coa indicate what type of mesh is used for the discretization. The collection of discretization points on a mesh is called a *grid*. The number n_{sub} is assumed to be high enough so that $\boldsymbol{\rho}_{\text{fin}}$ resolves $\rho(r)$ to the precision sought in our computations.

8.2 Compression

The following decomposed low-rank approximation of the discretization of K° on the fine mesh holds to very high accuracy:

$$\mathbf{K}_{\text{fin}}^\circ \approx \mathbf{P} \mathbf{K}_{\text{coa}}^\circ \mathbf{P}_W^T. \quad (53)$$

Here $\mathbf{K}_{\text{fin}}^\circ$ is a $(256 + 96n_{\text{sub}}) \times (256 + 96n_{\text{sub}})$ matrix, $\mathbf{K}_{\text{coa}}^\circ$ is a 256×256 matrix, \mathbf{P} is a prolongation matrix from the coarse grid to the fine grid and

$$\mathbf{P}_W = \mathbf{W}_{\text{fin}} \mathbf{P} \mathbf{W}_{\text{coa}}^{-1}, \quad (54)$$

where \mathbf{W} is a diagonal matrix containing the quadrature weights of the discretization, see [25, Section 5]. Superscript T denotes the transpose.

The relation (53) has powerful consequences for computational efficiency in the context of solving (52). As we soon shall see, it allows us to compress that equation and obtain the accuracy offered by the fine grid while working chiefly on the coarse grid. Only $(\mathbf{I} + \lambda \mathbf{K}^\star)^{-1}$ needs the fine grid for resolution. We introduce the compressed quadrature-weighted inverse

$$\mathbf{R} = \mathbf{P}_W^T (\mathbf{I}_{\text{fin}} + \lambda \mathbf{K}_{\text{fin}}^\star)^{-1} \mathbf{P}. \quad (55)$$

With (55), the discretization of (10) assumes the final form

$$(\mathbf{I}_{\text{coa}} + \lambda \mathbf{K}_{\text{coa}}^\circ \mathbf{R}) \tilde{\boldsymbol{\rho}}_{\text{coa}} = \lambda \mathbf{g}_{\text{coa}}, \quad (56)$$

where all matrices are 256×256 . For later reference we introduce

$$\hat{\boldsymbol{\rho}}_{\text{coa}} = \mathbf{R} \tilde{\boldsymbol{\rho}}_{\text{coa}} \quad (57)$$

as a *weight-corrected* density [30, Section 5].

8.3 Recursion

The compressed inverse \mathbf{R} has a block diagonal structure with four identical 64×64 blocks \mathbf{R}_k associated with the vertices s_k . The construction of a block \mathbf{R}_k from the definition (55) is costly when n_{sub} is large. Fortunately, this construction can be greatly sped up via a recursion. In general situations this recursion uses grids on hierarchies of local meshes, see [25, Section 6] and [26, Section 5]. For wedge-like corners, thanks to scale invariance of $K(r, r')$, only two local meshes \mathcal{M}_b and \mathcal{M}_c are needed, see right image of Fig. 1. The recursion for block \mathbf{R}_k assumes the form of a simple fixed-point iteration

$$\mathbf{R}_{ik} = \mathbf{P}_{Wbc}^T \left(\mathbb{F}\{\mathbf{R}_{(i-1)k}^{-1}\} + \mathbf{I}_b^\circ + \lambda \mathbf{K}_{bk}^\circ \right)^{-1} \mathbf{P}_{bc}, \quad i = 1, \dots, n_{\text{sub}}, \quad (58)$$

where $\mathbf{R}_{ik} = \mathbf{R}_k$ for $i = n_{\text{sub}}$. The quadrature weighted and unweighted prolongation matrices \mathbf{P}_{Wbc} and \mathbf{P}_{bc} act from a grid on a local mesh \mathcal{M}_c to a grid on a local mesh \mathcal{M}_b . The superscript \circ in (58) has a similar meaning as in (49) and the operator $\mathbb{F}\{\cdot\}$ expands a matrix by zero-padding, see [27, Section 6].

The derivation of (58) relies on a low-rank approximation similar to (53)

$$\mathbf{K}_a^\circ \approx \mathbf{P}_{ab} \mathbf{K}_b^\circ \mathbf{P}_{Wab}^T, \quad (59)$$

where \mathbf{K}_a is a discretization of K on a multiply refined local mesh \mathcal{M}_a . See [29, Section 7] for details. Conceptually, one could think of (58) as a process on a multiply refined local mesh, going outwards from the vertex, where step i inverts and compresses contributions to \mathbf{R}_k involving the outermost panels on level i .

The number n_{sub} needed for resolution of \mathbf{R}_k may grow without bounds as z approaches σ_{usq} (in infinite precision arithmetic). In order to accelerate the recursion we activate a combination of numerical homotopy and Newton's method when deemed worthwhile, see [27, Section 6]. The Newton iterations are continued until the relative update in \mathbf{R}_{ik} is smaller than $100\epsilon_{\text{mach}}$ or a maximum number of 20 iterations is reached, which roughly corresponds to a local mesh \mathcal{M}_a that is refined $n_{\text{sub}} \approx 2^{20} \approx 10^6$ times.

8.4 Solution, post-processing and interpretations

Once the 256×256 linear system (56) is solved for $\tilde{\rho}_{\text{coa}}$, various quantities of interest can be computed. For example, the polarizability (15) becomes

$$\alpha(z) = \mathbf{h}_{\text{coa}}^T \mathbf{W}_{\text{coa}} \mathbf{R} \tilde{\rho}_{\text{coa}}, \quad (60)$$

where \mathbf{h} is the discretization of $h(r)$. Results produced in this way are extremely accurate and fully confirm 24 of the entries for $\alpha(z)$ with $|z| \geq 1$ in Table 1 of [42]. The remaining 5 entries differ in the last digit. Section 8 of [27] gives error estimates for results produced in periodic settings.

The original density ρ_{fin} can be reconstructed from $\tilde{\rho}_{\text{coa}}$ by, in a sense, running the recursion (58) backwards (inwards on a multiply refined local mesh). If this process is interrupted part-way, one is left with a mix of discrete values of the original density ρ (on outer panels) and quantities which can be easily converted into discrete values of a weight-corrected density $\hat{\rho}$ (on the innermost panels). Details of the process are given in [25, Section 7]. Here it suffices to observe that there exists a rectangular matrix \mathbf{Y} , say, whose action on $\tilde{\rho}_{\text{coa}}$ produces entries of ρ_{fin} .

Let \mathbf{Q} denote a restriction matrix from the fine grid to the coarse grid. Then

$$\rho_{\text{coa}} = \mathbf{Q} \mathbf{Y} \tilde{\rho}_{\text{coa}} \quad (61)$$

and

$$\mathbf{K}_{\text{coa}}^{\circ} \mathbf{R} \tilde{\rho}_{\text{coa}} = \mathbf{K}_{\text{coa}}^{\circ} \mathbf{R} (\mathbf{Q} \mathbf{Y})^{-1} \rho_{\text{coa}}. \quad (62)$$

We see that the blocks of the block-diagonal matrix $\mathbf{R} (\mathbf{Q} \mathbf{Y})^{-1}$ have an interpretation as multiplicative weight corrections needed if $\mathbf{K}_{\text{coa}}^{\circ}$ is to act accurately on ρ_{coa} . Other useful interpretations of the matrices introduced include: The columns of \mathbf{Y} are discrete basis functions for $\rho(r)$ on the fine grid; The columns of \mathbf{R} are discrete basis functions for $\rho(r)$ on the coarse grid multiplied with quadrature weights; the rectangular matrix $\mathbf{Y} (\mathbf{Q} \mathbf{Y})^{-1}$ maps ρ_{coa} to ρ_{fin} . These observations will be used in what follows.

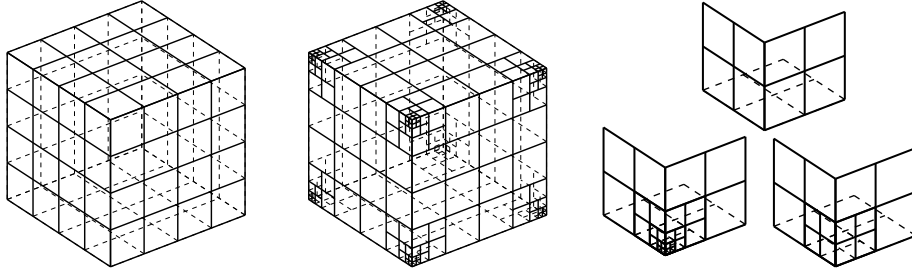


Figure 2: Meshes on the surface S of a cube. Left: the coarse mesh. Middle: a mesh that is refined $n_{\text{sub}} = 3$ times. Right: local meshes \mathcal{M}_a , \mathcal{M}_b and \mathcal{M}_c centered around a corner vertex. Compare Fig. 1

The machinery of Sections 8.1, 8.2 and 8.3 is useful in several ways. The preconditioning aspect of (56) reduces numerical error and improves the convergence of iterative solvers. The compression aspect of (56) saves degrees of freedom and makes the algorithm fast and memory efficient. The recursion (58) resolves the singular nature of $\rho(r)$ close to corner vertices in an automated fashion and provides efficient basis functions and quadrature weights contained in the matrix \mathbf{R} . No asymptotic analysis is required – we simply use Gauss-Legendre quadrature on the coarse mesh and on the local meshes \mathcal{M}_b and \mathcal{M}_c on which the recursion (58) takes place. Most, but not all, of these features can be retained as we step up into three dimensions.

9 Algorithm for the cube

Our algorithm for the cube mimics that of Section 8. A problem, however, arises in the split (49). Unlike the square, the cube has both sharp edges and sharp corners and it is not possible to identify suitably disjoint surface elements S_k^* that allow for an operator split $K = K^* + K^\circ$ where K° is a compact operator. Thus, one cannot construct a block-diagonal matrix \mathbf{R} which contains weighted basis functions for $\rho(r)$ that simultaneously resolve the singularities stemming from the edges and from the corners. We shall circumvent this difficulty by focusing solely on the cube corners and construct the coarse and the fine mesh with square quadrature panels according to Fig. 2, that is, in complete analogy with Fig. 1. As to compensate for the lack of refinement towards the edges, the discretization of K^* and K° will incorporate ready-made one-dimensional basis functions and weights constructed for a square with the same λ according to Section 8.4.

9.1 Preconditioning and discretization

This section is a counterpart to Section 8.1. Let the eight corner vertices of the cube be denoted s_k and introduce surface element S_k^* that cover the 12

quadrature panels on the coarse mesh that lie closest to s_k . Furthermore, let the smaller surface elements $S_k^{\star\star}$ be such that they cover the three panels on the coarse mesh that lie closest to s_k . The S_k^{\star} are disjoint, their union is S , and the kernel split (49) results in an operator split where the part of K° which accounts for interaction between points in $S \setminus S_k^{\star}$ and $S_k^{\star\star}$ is compact. This restricted compactness is sufficient for our purposes since mesh refinement only takes place on the $S_k^{\star\star}$, see the middle image of Fig. 2.

We discretize (10) and make the change of variables that leads to (52). The discretization of K proceeds in three steps. First, we use the Nyström method applying tensor products of n_p -point Gauss–Legendre quadrature formulas on all quadrature panels to get an initial \mathbf{K} . Then, for columns of \mathbf{K} acting on discrete densities on panel pairs neighboring a single cube edge, but not a corner, we correct the Gauss–Legendre weights in the direction perpendicular to the edge. These corrections are realized by multiplying submatrices of \mathbf{K} with blocks of $\mathbf{R}_{\text{sq}} (\mathbf{Q}_{\text{sq}} \mathbf{Y}_{\text{sq}})^{-1}$, where subscript sq indicates the square. See Section 8.4. This is our *basic discretization*. The resulting \mathbf{K} acts accurately on ρ in situations describing the convolution of $K(r, r')$ with $\rho(r')$ both for r' away from edges and corners and for r' close to an edge but away from corners and r away from r' .

Lastly, we change blocks of \mathbf{K} describing interaction between panel pairs neighboring each other on opposite sides of an edge. Such interaction requires special attention due to the non-smooth nature of $K(r, r')$ close to edges. We use interpolatory quadrature based on polynomial basis functions in the direction parallel to the edge and on the basis functions of \mathbf{Y}_{sq} in the direction perpendicular to the edge. This gives our final \mathbf{K} . The total number of discretization points on the coarse mesh is $n = 96n_p^2$. The fine mesh has $(96 + 72n_{\text{sub}})n_p^2$ points.

The choice of the columns of \mathbf{Y}_{sq} as discrete basis functions for $\rho(r)$ in the direction perpendicular to edges should be asymptotically correct, assuming that the singularities $\rho(r)$ are dominated by two-dimensional effects away from the corner. Still, these basis functions are not optimal and they are responsible for the slower rate of convergence that we shall see when solving (56) for the cube, compared to when solving (56) for the square.

9.2 Compression, recursion and post-processing

The compression of (52) for the cube is analogous to that for the square in Section 8.2. The only difference, apart from that various matrices have different sizes, is that \mathbf{W} , which contains the quadrature weights of the basic discretization and enters into the definition of prolongation matrix \mathbf{P}_W of (54), is no longer diagonal. The blocks of $\mathbf{R}_{\text{sq}} (\mathbf{Q}_{\text{sq}} \mathbf{Y}_{\text{sq}})^{-1}$, used as multiplicative weight corrections, are generally full matrices.

The recursion for \mathbf{R} of the cube, from now on denoted \mathbf{R}_{cu} , follows Section 8.3 exactly. Some λ allow for a rapid convergence in (58). Other λ ,

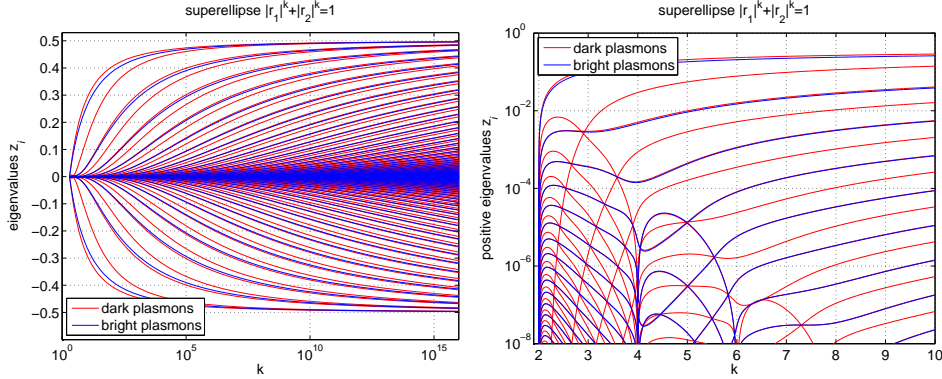


Figure 3: The eigenvalues z_i of K (locations of plasmons) for the superellipse varies with k . Left: z_i with $2 \leq k \leq 10^{16}$. The eigenvalue at -1 , a dark plasmon, is omitted. Right: zoom of positive eigenvalues with $2 \leq k \leq 10$.

corresponding to z close to parts of $\sigma_{\mu\text{cu}}$, require that we resort to Newton's method and numerical homotopy. Note that recursions are carried out twice in the scheme: both for \mathbf{R}_{sq} , needed for the discretization, and for \mathbf{R}_{cu} .

The polarizability $\alpha(z)$ of the cube can be computed from (60) once the $96n_p^2 \times 96n_p^2$ system (56) is solved. The matrix \mathbf{W}_{coa} in (60) is now weight-corrected as described in the first paragraph of this section. We use the GMRES iterative solver for (56) and make some use of symmetry in order to reduce memory requirements.

10 From circle to square

In a series of numerical experiments we now study the spectrum of K and the polarizability $\alpha(z)$ for a surface S that is gradually transformed from smooth to non-smooth. Such a study is of interest for several reasons. Due to the difficulties associated with solving electrostatic problems on non-smooth domains, see Section 7, it is common to round sharp boundary features prior to discretization [34, 54, 56]. Numerical effects, similar to those caused by rounding, could also result from insufficient resolution [47]. Furthermore, no edge or corner in real world physics is infinitely sharp and the degree of edge smoothness can be critical in the design of, for example, nanoantennas [21]. Finally, the experiments illustrate the theory overview of Section 3 in a setting which allows for high accuracy. All experiments are executed on a workstation equipped with an IntelCore2 Duo E8400 CPU at 3.00 GHz and 4 GB of memory.

Similar to Klimov [36] we let S be the superellipse

$$|r_1|^k + |r_2|^k = 1, \quad (63)$$

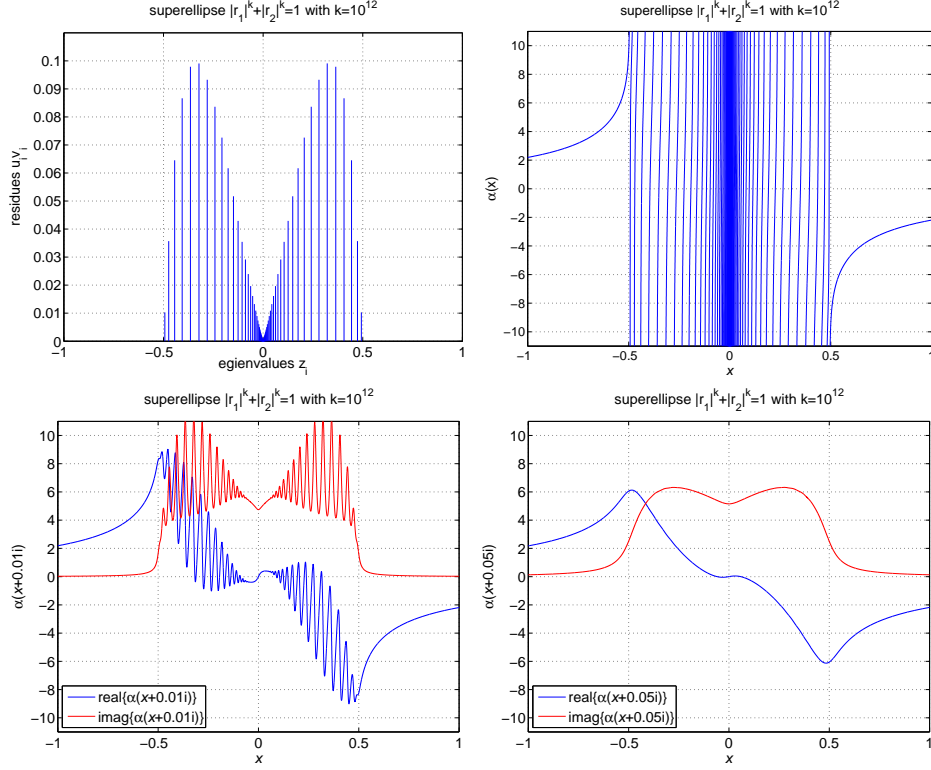


Figure 4: The number of eigenvalues z_i with comparatively large residues $u_i v_i$ for the superellipse (dominant plasmon modes) depends on k , and $\alpha(z)$ of (18) decays away from $z \in [-0.5, 0.5]$. Here $k = 10^{12}$. Upper left: the 208 largest residues. Upper right: $\alpha(x)$ with $x \in [-1, 1]$. Lower left: $\alpha(x+0.01i)$. Lower right: $\alpha(x+0.05i)$. Compare Figs. 3 and 5.

which for $k = 2$ is a circle and for $k \rightarrow \infty$ approaches a square. We first compute eigenvalues of K using a discretization based on composite 16-point Gauss–Legendre quadrature and adaptive mesh refinement. Particular care is taken in the parameterization of S as to allow for resolution at boundary portions of high curvature. The accuracy in these computations varies with k . A rough estimate is a relative error of $\log_{10}(k) \cdot \epsilon_{\text{mach}}$.

Eigenvalues and the nature of their corresponding plasmons are shown in Fig. 3. The only bright plasmon at $k = 2$ is a dipole. When $k > 2$, the bright plasmons have potential fields that are a mix of modes (dipoles, octupoles, etc.). The left image of Fig. 3 shows that K of the superellipse at $k = 10^{16}$, which is close to a square in double precision arithmetic, has a spectrum that does not look continuous to the eye. The right image of Fig. 3 zooms in on the spectrum at low k . Klimov [36], in an analogous study for a superellipsoid with $2 \leq k \leq 6$, observes a phase-transition at $k = 2.5$ and a critical point at $k \approx 3$.

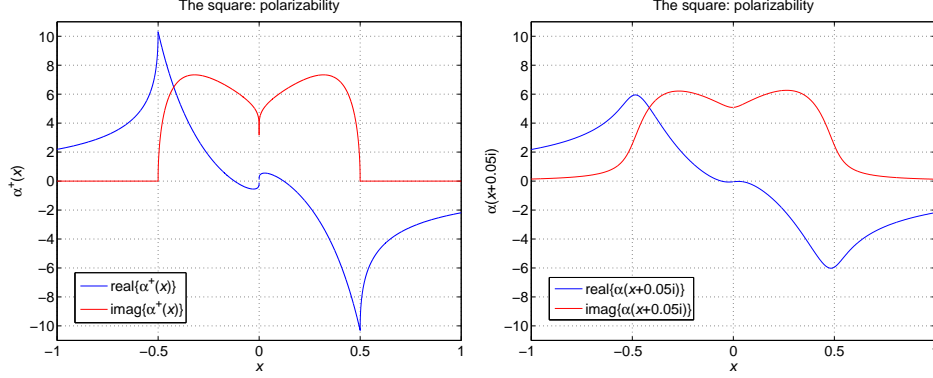


Figure 5: Polarizability of a square. Left: $\alpha^+(x)$. The curves are supported by 16492 data points whose relative accuracies range from machine precision to five digits. No convergent results were obtained within a distance of 10^{-7} from $x = 0$. The values of $\Re\{\alpha^+(x)\}$ at $x = \mp 0.5$ are ± 10.3121215292 . The sum rule (22), evaluated via (25) using a composite trapezoidal rule, holds to a relative precision of 10^{-6} . Right: $\alpha(x + 0.05i)$.

The number of eigenvalues z_i with comparatively large residues $u_i v_i$ in $\alpha(z)$ of (18) depends on k . Fig. 4 shows residues and polarizabilities $\alpha(z)$ for $k = 10^{12}$. Fig. 4 also shows how $\alpha(z)$ approaches a slowly varying function as z migrates from $\overline{\sigma_{\mu\text{sq}}} = [-0.5, 0.5]$.

Fig. 5 compares $\alpha^+(x)$ with $\alpha(x + 0.05i)$ for a square. The algorithm of Section 8 is used. Each data point takes only a fraction of a second to compute and is accurate almost to machine precision except for x very close to $\{-0.5, 0, 0.5\}$. For example, the relative difference between the computed value of $\alpha^+(1)$ and its known value $-\Gamma(\frac{1}{4})^4/8\pi^2$, see [52], is $2 \cdot 10^{-16}$. The left image of Fig. 5 shows that the square has no bright plasmons (no poles in $\alpha^+(x)$) and stands in forceful contrast the top right image of Fig. 4, which exhibits a myriad of plasmons for the superellipse at $k = 10^{12}$.

It is interesting to compare the right image of Fig. 5 with the lower right image of Fig. 4. Already at a distance of 0.05 away from the real axis, $\alpha(z)$ of the square and $\alpha(z)$ of the superellipse at $k = 10^{12}$ are similar, as to be expected in view of Theorem 5.7. The convergence as $k \rightarrow \infty$ is uniform in z in compact sets away from $[-1, 1]$. The accuracy achieved and the time required to evaluate $\alpha(z)$, however, are very different. While the accuracy in $\alpha(z)$ of the superellipse, computed via (18), is perhaps four digits and involves the eigenvalue decomposition of a 5376×5376 matrix, the accuracy in $\alpha(z)$ of the square, computed via (56), is much higher and involves only computations with matrices of size 256×256 . We conclude that even when corners need not be strictly sharp from a physical viewpoint, it pays off to keep them sharp from a numerical viewpoint.

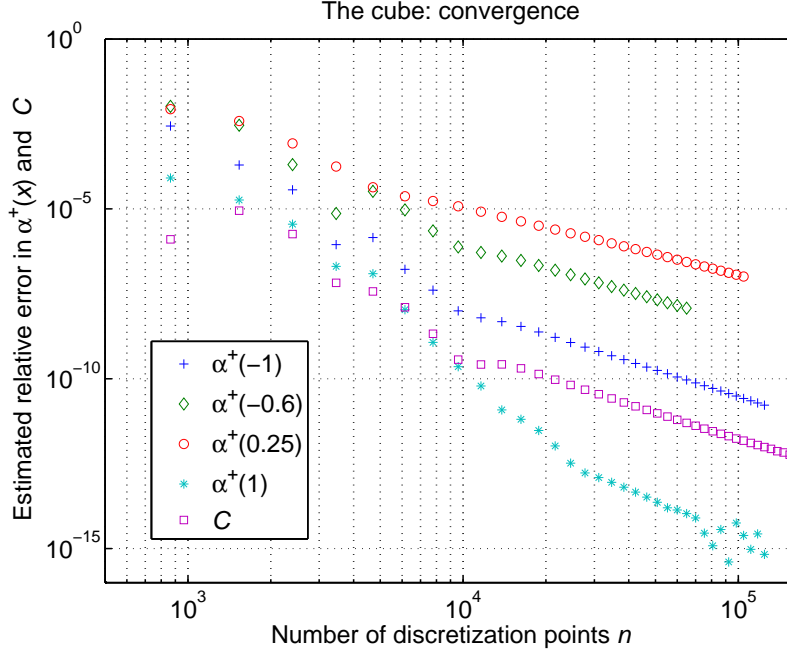


Figure 6: Convergence with the number of discretization points for the polarizability $\alpha^+(x)$ and capacitance C of a unit cube. The values of x correspond to: cube with infinite permittivity ($x = -1$), resonance in corners ($x = -0.6$), resonance along edges ($x = 0.25$), and cube with zero permittivity ($x = 1$). See Table 1 for reference values used in error estimates.

11 The cube

This section presents numerical results for the polarizability $\alpha^+(x)$ and capacitance C of the unit cube produced by the algorithm of Section 9. While computing C has a long history in computational electromagnetics [3, 33, 46], computing $\alpha^+(x)$ is less explored territory [51] that only recently, with the rapid growth of the field of nanotechnology, has become fashionable. For example, $\sigma_{\mu\text{cu}} = \{x : \mu'(x) > 0\}$ seems to be largely unknown. Fuchs [16] and Langbein [39], over thirty years ago, found six or eleven approximate eigenvalues for K of the cube (“major/dipole absorption peaks”) in the intervals $[-0.573, 0.408]$ and $[-0.586, 0.274]$, respectively and which supposedly account for around 95% of the sum (19). In view of the findings of the present paper, so far, one could suspect that these peaks are an artifact of insufficient resolution or unintended rounding of edges. Be as it may, this pioneering and highly cited work is now of interest in nanoplasmonics where the coupling of plasmon modes in metallic nanostructures such as nanocube dimers is important and interpretations seem to rely on these peaks [21, 36, 50, 56].

Table 1: Reference values, estimated relative errors, and best previous estimates for the limit polarizability $\alpha^+(x)$ and the capacitance C of the cube.

	present reference values	relerr	previous results	relerr
$\alpha^+(-1)$	3.644305190268	10^{-11}	3.6442 [51]	$3 \cdot 10^{-5}$
$\alpha^+(-0.6)$	$5.85574775 + 16.64205643i$	10^{-8}		
$\alpha^+(0.25)$	$-2.76289923 + 3.08034031i$	10^{-7}		
$\alpha^+(1)$	-1.63841571293652	10^{-13}	-1.6383 [51]	$6 \cdot 10^{-5}$
C	0.6606781540995	10^{-12}	0.66067813 [33]	10^{-7}

In our algorithm for $\alpha^+(x)$ via (56), a complex valued \mathbf{R} generally implies a complex valued solution $\tilde{\rho}_{\text{coa}}$, complex valued basis functions \mathbf{Y} , and $\Im\{\alpha^+(x)\} > 0$. The square exhibits complex valued limits of \mathbf{R}_{sq} whenever $z = x + iy \in \mathbb{C}_+ \rightarrow x \in \sigma_{\mu\text{sq}}$. The cube, which uses \mathbf{R}_{sq} and \mathbf{Y}_{sq} for the discretization of K and which in turn enters into the recursion (58) for \mathbf{R}_{cu} , will therefore have complex valued limits of \mathbf{R}_{cu} and $\Im\{\alpha^+(x)\} > 0$ whenever $x \in \sigma_{\mu\text{sq}}$. We refer to this as *resonance along edges*. The reason being that $\Im\{\alpha^+(x)\} > 0$ implies $x \in \text{Spec}(K, H^{-1/2})$ and, as a consequence of the symmetrization arguments in Section 5 and the fact that the spectrum of a self-adjoint operator consists of eigenvalues and approximate eigenvalues, each such x is either an eigenvalue or an approximate eigenvalue of K on $H^{-1/2}(S)$. Moreover, \mathbf{R}_{cu} may remain complex valued throughout the numerical homotopy process as $z = x + iy \in \mathbb{C}_+ \rightarrow x$ for other $x \in [-1, 1]$ as well, that is, where limits of \mathbf{R}_{sq} are real valued. We refer to this as *resonance in corners*.

Fig. 6 shows results from convergence tests. The total number of discretization points on the cube surface is n . The examples with $n \gtrsim 2 \cdot 10^4$ were executed on a workstation equipped with an IntelXeon E5430 CPU at 2.66 GHz and 32 GB of memory. Out of the chosen values of x , one can see that the error in $\alpha^+(x)$ is largest for $x = 0.25$. This is not surprising. A weakness in our algorithm is the assumption that the columns of \mathbf{Y}_{sq} are efficient basis functions for $\rho(r)$ in the direction perpendicular to an edge. When $x = 0.25$, there is resonance along edges and the shortcomings of this assumption should be particularly visible. When $x = -1$, $x = 1$ and for C there are real valued solutions $\rho(r) \in L^2(S)$ which are easier to resolve.

The recursion (58) for \mathbf{R}_{cu} requires a substantial amount of memory when n_{p} is large and Newton's method is activated. This explains why the test series for $\alpha^+(-0.6)$ in Fig. 6 had to be interrupted at $n = 64896$, that is, for $n_{\text{p}} = 26$. Timings vary greatly with x , n_{p} , and the error tolerances that are set in recursions and iterative solvers. For safety, we set tolerances low and quote the following approximate computing times for $n = 9600$:

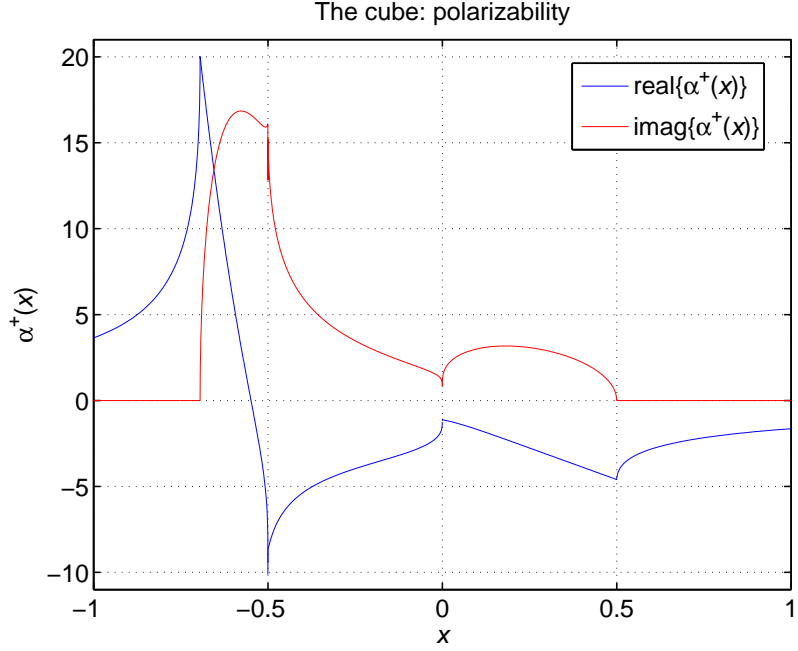


Figure 7: Polarizability of a cube. The curves are supported by 1195 data points whose relative accuracies range from ten to five digits. No convergent results were obtained for $\alpha^+(x)$ within a distance of 10^{-10} from $x = -0.5$ and within a distance of 10^{-5} from $x = 0$. The maximum value of $\Re\{\alpha^+(x)\}$ is 20.00826 and occurs at $x \approx -0.694526$. The sum rules (22), (23), and (64), evaluated via (25) using a composite trapezoidal rule, hold to a relative precision of $3 \cdot 10^{-5}$, $4 \cdot 10^{-5}$, and $6 \cdot 10^{-5}$, respectively.

$\alpha^+(-1)$, $\alpha^+(1)$, and C took one minute each; $\alpha^+(0.25)$ took two minutes; $\alpha^+(-0.6)$ took ten minutes. The test series for $\alpha^+(-1)$, $\alpha^+(1)$ and C all confirm previous available results, see Table 1, and improve on these with between five and eight digits.

Fig. 7 is our main numerical result. It shows that the isolated cube has no bright plasmons (no poles in $\alpha^+(x)$). For validation, see the figure caption, we have used the two sum rules (22), (23) and a third sum rule

$$\int_{\mathbb{R}} x^2 \mu'(x) dx = 0.433464767896, \quad (64)$$

which has been determined numerically for the cube [24]. Fig. 7 also shows that $\sigma_{\mu\text{cu}}$ is approximately equal to the interval $(-0.694526, 0.5)$, possibly punctured at $\{-0.5, 0\}$, and raises the intriguing question of what surface shapes S lead to connected σ_{μ} . Our computed $\sigma_{\mu\text{cu}}$ is broader than those estimated by earlier investigators [16, 36, 39] using other techniques. We conclude, again, that working with sharp edges and corners is an advantage.

12 Conclusions and outlook

We have constructed an electrostatic solver for cube-shaped domains and used it to produce new results for some canonical problems. A particular characteristic of the solver is that it takes advantage of sharp edges and corners, rather than being a victim of them.

A mathematical framework capturing the symmetric features of the double layer potential and its adjoint has been identified, allowing for analysis of the polarizability $\alpha(z)$ through spectral theory for self-adjoint operators. Moreover, this framework and its corresponding machinery is natural and satisfactory also from a physical viewpoint, as the potentials produced to solve the electrostatic problem are exactly those of finite energy. With full mathematical rigor we have shown how to, with respect to polarizabilities, interpret the limit process which occurs when deforming a smooth surface into a cube, a point which has generated a fair amount of discussion in the materials science community.

Furthermore, we have shown that while the polarizability via limits can be extended to a function $\alpha^+(x)$ defined almost everywhere on the real axis, the same statement fails for the corresponding potentials whenever the representing measure μ has a non-zero absolutely continuous part. That is, the potential corresponding to a point $x \in \mathbb{R}$ where $\mu'(x) > 0$ exists and is non-zero can not be given an interpretation neither as a limit from the upper half-plane, nor as a direct solution to the electrostatic problem.

For the cube, the mathematical theory in conjunction with the numerical findings show that $d\mu(x) = \mu'(x) dx$ is purely absolutely continuous, and that the set where $\mu'(x) > 0$ is given by the interval $(a, b) \approx (-0.694526, 0.5)$, possibly excepting the two points $x = -0.5$ and $x = 0$. Hence the integral representation (42) for $\alpha(z)$, in terms of $\mu'(x)$, holds. Finally, $\mu'(x)$ has been determined numerically. These discoveries, we hope, will be of use in plasmonics where absorption peaks of nanocubes play an important role.

Future efforts will be directed towards solving the Helmholtz equation, compare [4, 5, 6]. Should the polarizability of clusters of cubes or the effective permittivity of cubes in periodic arrangements be of interest, our solver requires only minor modifications.

Acknowledgements

We thank professors Alexandru Aleman, Anders Karlsson, Daniel Sjöberg, and Laurian Suciu for useful conversations.

References

- [1] R. A. Adams, ‘Sobolev spaces’, Pure and Applied Mathematics, Vol. **65**. Academic Press, New York-London, 1975.

- [2] D. Bergman, ‘The dielectric constant of a simple cubic array of identical spheres’, *J. Phys. C: Solid State Phys.*, **12**, 4947–4960 (1979).
- [3] Y.I. Bontzios, M.G. Dimopoulos, and A.A. Hatzopoulos, ‘An evolutionary method for efficient computation of mutual capacitance for VLSI circuits based on the method of images’, *Simul. Model. Pract. Th.*, **19**, 638–648 (2011).
- [4] J. Bremer, ‘A fast direct solver for the integral equations of scattering theory on planar curves with corners’, *J. Comput. Phys.*, **231**, 1879–1899 (2012).
- [5] J. Bremer, ‘On the Nyström discretization of integral equations on planar curves with corners’, *Appl. Comput. Harmon. Anal.*, **32**, 45–64 (2012).
- [6] J. Bremer, V. Rokhlin, and I. Sammis, ‘Universal quadratures for boundary integral equations on two-dimensional domains with corners’, *J. Comput. Phys.*, **229**, 8259–8280 (2010).
- [7] O.P. Bruno, J.S. Oval, and C. Turc, ‘A high-order integral algorithm for highly singular PDE solutions in Lipschitz domains’, *Computing*, **84**, 149–181 (2009).
- [8] J. A. Cima, A. L. Matheson, W. T., ‘The Cauchy transform’, *Mathematical Surveys and Monographs*, **125**. American Mathematical Society, Providence, RI, 2006.
- [9] R. R. Coifman, A. McIntosh, Y. Meyer, ‘L’intégrale de Cauchy définit un opérateur borné sur L^2 pour les courbes lipschitziennes’, (French), *Ann. of Math. (2)* **116** (1982), no. 2, 361–387
- [10] R.V. Craster and Yu.V. Obnosov, ‘Four-Phase Checkerboard Composites’, *SIAM J. Appl. Math.* **61**, 1839–1856 (2001).
- [11] L.C. Davis, ‘Electrostatic edge modes of a dielectric wedge’, *Phys. Rev. B.*, **14**, 5523–5525 (1976).
- [12] R. G. Douglas, ‘On majorization, factorization, and range inclusion of operators on Hilbert space’, *Proc. Amer. Math. Soc.* **17** 1966 413–415.
- [13] L. Escauriaza, E. B. Fabes, G. Verchota, ‘On a regularity theorem for weak solutions to transmission problems with internal Lipschitz boundaries’, *Proc. Amer. Math. Soc.* **115** (1992), no. 4, 1069–1076.
- [14] E. Fabes, O. Mendez, M. Mitrea, ‘Boundary layers on Sobolev-Besov spaces and Poisson’s equation for the Laplacian in Lipschitz domains’. *J. Funct. Anal.* **159** (1998), no. 2, 323–368.
- [15] E. Fabes, M. Sand, J. K. Seo, ‘The spectral radius of the classical layer potentials on convex domains’, *Partial differential equations with minimal smoothness and applications* (Chicago, IL, 1990), 129–137, *IMA Vol. Math. Appl.*, **42**, Springer, New York, 1992.
- [16] R. Fuchs, ‘Theory of the optical properties of ionic crystal cubes’, *Phys. Rev. B*, **11**, 1732–1739 (1975).
- [17] R. Fuchs and S. H. Liu, ‘Sum rule for the polarizability of small particles’, *Phys. Rev. B*, **14**, 5521–5522 (1976).

- [18] E. Gagliardo, ‘Caratterizzazioni delle tracce sulla frontiera relative ad alcune classi di funzioni in n variabili’, (Italian) Rend. Sem. Mat. Univ. Padova **27** 1957 284–305.
- [19] G. Geymonat, ‘Trace theorems for Sobolev spaces on Lipschitz domains. Necessary conditions’, Ann. Math. Blaise Pascal **14** (2007), no. 2, 187–197.
- [20] K. Golden and G. Papanicolaou, ‘Bounds for effective parameters of heterogeneous media by analytic continuation’, Comm. Math. Phys. Volume **90**, no. 4 (1983), 473–491.
- [21] N. Grillet, D. Manchon, F. Bertorelle *et al.* ‘Plasmon Coupling in Silver Nanocube Dimers: Resonance Splitting Induced by Edge Rounding’, ACS NANO, **5**, 9450–9462.
- [22] P. Grisvard, ‘Elliptic problems in nonsmooth domains’, Monographs and Studies in Mathematics, **24**. Pitman (Advanced Publishing Program), Boston, MA, 1985.
- [23] S. Hassi, Z. Sebestyén, H. S. V. de Snoo, ‘On the nonnegativity of operator products’, Acta Math. Hungar. **109** (2005), no. 1-2, 1–14,
- [24] J. Helsing, ‘Third-order bounds on the conductivity of a random stacking of cubes’, J. Math. Phys., **35**, 1688–1692 (1991).
- [25] J. Helsing, ‘Integral equation methods for elliptic problems with boundary conditions of mixed type’, J. Comput. Phys., **228**, 8892–8907 (2009).
- [26] J. Helsing, ‘A fast and stable solver for singular integral equations on piecewise smooth curves’, SIAM J. Sci. Comput., **33**, 153–174 (2011).
- [27] J. Helsing, ‘The effective conductivity of arrays of squares: large random unit cells and extreme contrast ratios’, J. Comput. Phys., **230**, 7533–7547 (2011).
- [28] J. Helsing, R.C. McPhedran, and G.W. Milton, ‘Spectral super-resolution in metamaterial composites’, New J. Phys. **13**, 115005, (2011).
- [29] J. Helsing and R. Ojala, ‘Corner singularities for elliptic problems: Integral equations, graded meshes, quadrature, and compressed inverse preconditioning’, J. Comput. Phys., **227**, 8820–8840 (2008).
- [30] J. Helsing and R. Ojala, ‘Elastostatic computations on aggregates of grains with sharp interfaces, corners, and triple-junctions’, Int. J. Solids Struct., **46**, 4437–4450 (2009).
- [31] J.H. Hetherington and M.F. Thorpe, ‘The conductivity of a sheet containing inclusions with sharp corners’, Proc. R. Soc. Lond. A, **438**, 591–604 (1992).
- [32] S. Hofmann, M. Mitrea, M. Taylor, ‘Singular integrals and elliptic boundary problems on regular Semmes-Kenig-Toro domains’, Int. Math. Res. Not. IMRN 2010, no. **14**, 2567–2865.
- [33] C.-O. Hwang, M. Mascagni, and T. Won, ‘Monte Carlo methods for computing the capacitance of the unit cube’, Math. Comput. Simulat., **80**, 1089–1095 (2010).
- [34] H. Kettunen, H. Wallén, and A. Sihvola, ‘Electrostatic resonances of negative-permittivity hemisphere’, J. Appl. Phys., **103**, 094112 (2008).

- [35] D. Khavinson, M. Putinar, H. S. Shapiro, ‘Poincaré’s variational problem in potential theory’, *Arch. Ration. Mech. Anal.* **185** (2007), no. 1, 143–184.
- [36] V.V. Klimov, Ya.N. Istomin, and Yu.A. Kosevich, ‘Plasma phenomena in nanostructures and neutron stars’, *Physics–Uspekhi*, **51**, 839–859 (2008).
- [37] P. Koosis, ‘Introduction to Hp spaces. Second edition. With two appendices by V. P. Havin’, *Cambridge Tracts in Mathematics*, **115**. Cambridge University Press, Cambridge, 1998.
- [38] M. G. Krein, ‘Compact linear operators on functional spaces with two norms’, Dedicated to the memory of Mark Grigorievich Krein (1907–1989). *Integral Equations Operator Theory* **30** (1998), no. 2, 140–162.
- [39] D. Langbein, ‘Normal modes at small cubes and rectangular particles’, *J. Phys. A: Math. Gen.*, **9**, 627–644 (1976).
- [40] I.D. Mayergoyz, D. R. Fredkin, and Z. Zhang, ‘Electrostatic (plasmon) resonances in nanoparticles’, *Phys. Rev. B*, **72**, 155412 (2005).
- [41] Y. Meyer, ‘Ondelettes et opérateurs. II.’, *Opérateurs de Calderón-Zygmund. Actualités Mathématiques*. Hermann, Paris, 1990.
- [42] G.W. Milton, R.C. McPhedran, and D.R. McKenzie, ‘Transport properties of arrays of intersecting cylinders’, *Appl. Phys.*, **25**, 23–30 (1981).
- [43] G.W. Milton, ‘Proof of a conjecture on the conductivity of checkerboards’, *J. Math. Phys.*, **42**, 4873–4882 (2001).
- [44] D. Mitrea, ‘The method of layer potentials for non-smooth domains with arbitrary topology’, *Integral Equations Operator Theory* **29** (1997), no. 3, 320–338.
- [45] I. Mitrea, ‘On the spectra of elastostatic and hydrostatic layer potentials on curvilinear polygons’, *J. Fourier Anal. Appl.* **8** (2002), no. 5, 443–487.
- [46] S. Mukhopadhyay and N. Majumdar, ‘A study of three-dimensional edge and corner problems using the neBEM solver’, *Eng. Anal. Bound. Elem.*, **33**, 105–119 (2009).
- [47] W.T. Perrins and R.C. McPhedran, ‘Metamaterials and the homogenization of composite materials’, *Metamaterials* **4**, 24–31 (2010).
- [48] M. Pitkonen, ‘A closed-form solution for the polarizability of a dielectric double half-cylinder’, *J. Electromagnet. Wave.*, **24**, 1267–1277 (2010).
- [49] F.H. Read, ‘Capacitances and singularities of the unit triangle, square, tetrahedron and cube’, *COMPEL*, **23**, 572–578 (2004).
- [50] R. Rupp, ‘Plasmon frequencies of cube shaped metal clusters’, *Z. Phys. D.*, **36**, 69–71 (1996).
- [51] A. Sihvola, P. Ylä-Oijala, S. Järvenpää, and J. Avelin, ‘Polarizabilities of Platonic Solids, *IEEE Trans. Antennas Propagat.*’, **52**, 2226–2233 (2004).
- [52] M.F. Thorpe, ‘The conductivity of a sheet containing a few polygonal holes and/or superconducting inclusions’, *Proc. R. Soc. Lond. A*, **437**, 215–227 (1992).

- [53] G. Verchota, ‘Layer potentials and regularity for the Dirichlet problem for Laplace’s equation in Lipschitz domains’, *J. Funct. Anal.* **59** (1984), no. 3, 572–611.
- [54] H. Wallén, H. Kettunen, and A. Sihvola, ‘Surface modes of negative-parameter interfaces and the importance of rounding sharp corners’, *Metamaterials*, **2**, 113–121 (2008).
- [55] J. Weidmann, ‘Strong operator convergence and spectral theory of ordinary differential operators’, *Univ. Iagel. Acta Math. No.* **34** (1997), 153–163.
- [56] S. Zhang, K. Bao, N.J. Halas, H. Xu, and P. Nordlander, ‘Substrate-Induced Fano Resonances of a Plasmonic Nanocube: A Route to Increased-Sensitivity Localized Surface Plasmon Resonance Sensors Revealed’, *Nano Lett.*, **11**, 1657–1663 (2011).